IN THE UNITED STATES PATENT AND TRADEMARK OFFICE

Patent Application No. 10/754,390

Confirmation No. 7753

Applicant: Prasad et al.

Filed: January 9, 2004

TC/AU: 3727

Examiner: Muller, Bryan R.

Docket No.: 100196 (Leydig Reference No. 223279)

Customer No.: 29050

Commissioner for Patents
P.O. Box 1450
Alexandria, VA 22313-1450

DECLARATION UNDER 37 C.F.R. § 1.132 OF ABANESHWAR PRASAD

I, Abaneshwar Prasad, hereby declare that:

1.   I am employed by Cabot Microelectronics Corporation. I am the inventor, along with my colleague Ronald Myers, of the subject matter disclosed and claimed in the subject patent application (hereinafter "our invention").

2.   I have a Ph.D. in polymer physics from Florida State University and was a National Science Foundation post-doctoral research and teaching fellow at Virginia Polytechnic Institute and State University. I have worked in industry since 1992. I was employed as a senior research scientist at Equistar Chemical Company for over eight years (now LyondellBasel) and have been employed at Cabot Microelectronics Corporation as a senior scientist for over ten years. I have published more than 25 articles and book chapters relating to various aspects of polymer physics. I have seventeen United States Patents issued to my name.

3.   I previously submitted two declarations during prosecution of the pending patent application. See "Declaration Under 37 C.F.R. § 1.132 of Abaneshwar Prasad" dated June 1, 2005, and "Declaration Under 37 C.F.R. § 1.132 of Abaneshwar Prasad" dated March 8, 2006.

4.   As described in my previous Declaration dated June 1, 2005, all known porous polymeric materials have a positive Poisson's ratio unless they are specially treated so as to convert them into a material having a negative Poisson's ratio. See Lee et al., "Anisotropic Polyurethane Foam With Poisson's Ratio Greater Than One," *Journal of Materials Science, 32*: 2397 (1997), attached as Exhibit A. As such, porous polymeric materials having a negative Poisson's ratio are uncommon. In fact, such materials were generally thought to be impossible to prepare until 1987 when Dr. Lakes reported the preparation of such negative Poisson's ratio materials by subjecting a conventional polymeric foam to triaxial compression combined with heating in a mold to a temperature slightly above the softening temperature of the polymeric foam. See Lakes et al., "Foam Structures with a Negative Poisson's Ratio," *Nature, 235*: 1038 (1987), attached as Exhibit B.

5.   To my knowledge, the use of a porous polymeric material having a negative Poisson's ratio in a polishing pad was not known prior to our invention.

6.   Moreover, the compression and temperature conditions necessary to convert a porous polymeric material having a positive Poisson's ratio to a porous polymeric material having a negative Poisson's ratio are not consistent with conventional processes for making polishing pads that were known at the time of our invention. In particular, a porous, polymeric material must be placed in a mold, tri-axially compressed (in the x, y, and z dimensions) to between 60% and 80% of its original size, heated to above the softening temperature of the material (e.g., to a temperature between 160° C and 210° C), held at that temperature for a period of time ranging from a few minutes to an hour, and then allowed to cool to room temperature while still in the mold. Conventional processes that were known in the art for making polishing pads at the time of our invention utilize, for example, (1) polymerization of liquid pre-polymer *in-situ* at polymerization temperatures of below 100° C without the application of pressure, (2) application of a super-critical gas to a polymer sheet to create pores in the polymer at high temperatures and pressures, (3) solid sheet (non-porous) extrusion, (4) sintering, and (5) solvent/non-solvent coagulation. Not only is the use of the triaxial compression and temperature conditions necessary for the creation of a negative Poisson's ratio material inconsistent with the conventional methods for making polishing pads, but the application of these conditions to many conventional polishing pads (e.g., polishing pads comprising non-porous solid polymeric materials) would not necessarily produce a negative Poisson's ratio material, because the materials utilized in the polishing pad may not possess the special characteristics that allow porous polymeric materials to be compressed in each of the three dimensions.

7.   Prior to our invention, there were several known methods to improve the abrasion resistance of polishing pads. For example, U.S. Patent 5,094,670 discloses a process for making a polishing pad wherein a nonwoven fabric of a synthetic fiber is impregnated with a polyurethane solution in order to improve abrasion. U.S. Patent 5,736,453 discloses the use of shape memory materials to densify the polishing pad in order to decrease wear over the life of the polishing pad. U.S. Patents 6,454,634 and 6,582,283 teach synthetic and/or chemical modifications of pad materials to improve impact resistance and pad wear and abrasion resistance. Prior to our invention, the potential impact on abrasion resistance of a porous polymeric material having a negative Poisson's ratio was not known.

8.   While polishing pads must exhibit sufficient abrasion resistance to withstand polishing processes, polishing pads must not exhibit so much abrasion resistance that they are resistant to conditioning processes that utilize abrasion to remove build-up that accumulates during polishing processes. A polishing pad with too much abrasion resistance may not be able to be adequately conditioned and, therefore, could lose polishing activity. Prior to our invention, there was no way to know whether a porous polymeric material modified to have a negative Poisson's ratio would provide the appropriate level of abrasion resistance necessary for good polishing activity.

9.   While conventional porous polymeric material having a positive Poisson's ratio *contracts* laterally when stretched, a porous polymeric material having a negative Poisson's ratio *expands* laterally when stretched.

10.   In particular, a conventional polymer material having a *positive* Poisson's ratio resists a change in volume more than it resists a change in shape. As such, when a conventional polymer material having a positive Poisson's ratio is stretched, it contracts laterally. This contraction places considerable stress on the polymer chains within the polymer material. This increase in stress due to contraction can be observed in a stress-strain curve and is referred to as strain-hardening. Specifically, when the polymeric material contracts laterally (after any elastic deformation), the stress-strain curve rises substantially reflecting the increase in stress placed on the polymer chains in the material. The increase continues until the breaking point. For conventional polymeric materials having a positive Poisson's ratio, the increase in stress (and subsequent rise in the stress-strain curve) can occur just following the yield point or shortly thereafter depending on whether the material is crystalline, cross-linked, or amorphous.

11.   A polymer material having a *negative* Poisson's ratio resists a change in shape more than it resists a change in volume. As such, materials having a negative Poisson's ratio do

not contract laterally when they are stretched. Rather, these materials expand laterally when stretched and contract when compressed. Because the polymeric material does not contract laterally, there is no stress placed on the polymer chains within the polymeric material. As a result, polymeric materials having a negative Poisson's ratio have a markedly different stress-strain curve. Eventually all polymeric materials undergo some strain hardening; however, the strain hardening is significantly delayed in polymeric materials having a negative Poisson's ratio. This means that a stress-strain curve for a negative Poisson's ratio material does not show a marked rise following the yield point but will remain substantially flat as the strain is increased. This flat portion reflects the fact that the polymeric material is not contracting laterally and thereby placing stress on the polymer chains, but rather is expanding. See F. Scarpa et al., "Passive and MR-Fluid Coated Auxetic Foam - Mechanical and Electromagnetic Properties," *Journal of Intelligent Material Systems and Structures*, *15*: 973 (2004), attached as Exhibit C; as well as Friis et al., "Negative Poisson's Ratio Polymeric and Metallic Foams," *Journal of Materials Science*, *23*: 4406 (1998), attached as Exhibit D.

12.   The differentiating behavior of negative Poisson's ratio material provides increased resiliency to the porous polymeric material, which creates many benefits in chemical-mechanical polishing applications that were previously unavailable in the art. When a material having a negative Poisson's ratio is subjected to stresses, including those imposed on the polishing pad during polishing processes, the material will display greater durability and less deformation.

13.   Conventional polishing pads use macrotexture (e.g, grooves), microtexture (e.g., texture created by diamond conditioning disks), and porosity as vehicles to absorb and transport slurry (see, e.g., U.S. Patents 5,489,233; 6,217,434; 6,287,185). While such pad materials are susceptible to plastic deformation and glazing due to accumulation of polishing debris, efficient replenishment of the polishing surface is achieved by abrasion of the pad surface material via diamond conditioning. Diamond conditioning, however, can shorten pad life due to excessive removal of the pad surface material. Insufficient conditioning, on the other hand, can also shorten pad life due to glazing. Unlike conventional polishing pads, the use of a porous polymeric material having a negative Poisson's ratio in a polishing pad allows for self-cleaning during polishing processes, which increases pad durability and pad life. The cells (i.e., pores) of a negative Poisson's ratio material are formed into a "re-entrant" shape, which bulges inwards and unfolds under tension, thereby resulting in a lateral expansion. This "re-entrant" cell structure improves the flow of the slurry during polishing and reduces the need for diamond pad conditioning because the polishing debris have less tendency to accumulate on the pad surface

(re-entrant cell structure allows absorption of by-products that can be simply washed away by high pressure water rinse in between polishing steps), thereby resulting in increased pad life.

14.   In addition, the use of a porous polymeric material having negative Poisson's ratio results in a polishing pad having improved stress distribution and shock absorbing capabilities, which makes the pad less likely to deform with increased polishing. Because the process used to create a negative Poisson's ratio material increases the density of the material, the resulting material is stronger and better able to absorb shocks and stresses that can result from polishing processes. Such materials exhibit a nearly linear relationship between compressive stress and strain, and can strain up to 40% with no abrupt collapse of cell structure, thereby making a polishing pad containing this material more resilient and less deformable under compression than conventional polishing pads. See Lakes et al., "Foam Structures with a Negative Poisson's Ratio," *Nature*, *235*: 1038 (1987), attached as Exhibit B. Less pad deformation results in more uniform polishing throughout the life of the pad with improved planarization.

15.   Moreover, the improved resilience of a polishing pad containing a negative Poisson's ratio material will reduce "edge-on" effects during polishing processes. Specifically, such a polishing pad is able to better withstand the impact forces that result when the polishing pad contacts a wafer. A polishing pad comprising negative Poisson's ratio material is sufficiently compliant that it is able to distribute concentrated force, but also sufficiently rigid that it will not compress despite the force. A conventional porous polymeric material that has not been modified to have a negative Poisson's ratio does not show any particular resilience under stress. See F. Scarpa et al., "Passive and MR-Fluid Coated Auxetic Foam - Mechanical and Electromagnetic Properties," *Journal of Intelligent Material Systems and Structures*, *15*: 973 (2004), attached as Exhibit C.

16.   I hereby declare that all statements made herein of my own knowledge are true, that all statements made on information and belief are believed to be true, that these statements were made with the knowledge that willful false statements and the like so made are punishable by fine or imprisonment, or both, under Section 1001 of Title 18 of the United States Code, and that such willful false statements may jeopardize the validity of the application or any patent issued thereon.

Date: June 21, 2011   _____
                                                        Abaneshwar Prasad

EXHIBIT A

Anisotropic polyurethane foam
with Poisson's ratio greater than 1

Abstract

Anisotropic polymer foams have been prepared, which exhibit a Poisson's ratio exceeding 1, and ratios of longitudinal to transverse stiffness exceeding 50. The foams are as much as 20 times stiffer in the longitudinal direction than the foams from which they were derived. The transformation process involved applying a uniaxial stress sufficient to produce 25% to 45% axial strain to open-cell polyurethane foam, heating above the softening point, followed by cooling under axial strain.

1.   Introduction

A cellular material is one made up of an interconnected network of solid struts or plates which form edges and faces of cells. It may be viewed as a composite consisting of a solid phase and empty space or a fluid phase such as air. Cellular solids have served structural roles in nature as honeycombs, bone and coral skeletons, for millions of years. Man, on the other hand, has only recently begun to realize the potential of these materials and has made an attempt to utilize their structure-property relations in practical applications.

Cellular solids, including foams, are very efficient structures in terms of optimizing strength and stiffness with respect to weight. Foam materials have often been called "nature's equivalent of the I-beam" [1], and are commonly employed in cushioning, insulating, padding and packing et al. Encouraged by the engineering potential of cellular materials, one is motivated to understand the mechanical behavior of the cellular solid.

All commonly known cellular materials (naturally existing and man-made), have a convex cell shape and exhibit a positive Poisson's ratio which is defined as the negative of the lateral strain divided by the axial strain when a load is applied in an axial direction. Such materials undergo a lateral contraction in response to an axial stretch, and a lateral expansion when subjected to axial compression. Therefore, for all ordinary materials, Poisson's ratio has a positive value. For reference, typical Poisson's ratios for some common material are 0.5 for rubbers, 0.33 for aluminum, 0.27 for most steels, 0.1 to 0.4 for typical polymeric foams, and nearly zero for cork [2].

The theoretical allowable range of Poisson's ratio for isotropic materials in three dimensions is -1 to 0.5 as demonstrated by energy arguments [3]. An isotropic material with negative Poisson's ratio, however, was not believed to exist until recent work by Lakes [4]. The fabrication was achieved through a transformation of the cell structure from a convex polyhedral shape to a concave shape. These types of foam samples having a negative Poisson's ratio have been termed "re-entrant" due to their macrostructural appearance and behavior. Prior experiments in preparing and studying re-entrant polyurethane foam (Scott industrial foam) [4, 5, 6], silicone rubber foam [5] and metal foam [4, 5, 7] dealt with open-cell foam. Different techniques were used for each of these materials.

In this study, an open-cell polyurethane foam was strained in tension at elevated temperature, resulting in characteristic permanent transformations. Scott Industrial foam with a pore size 0.4 mm (65 pores per inch (ppi)) was used. This is similar, except for pore size, to the Scott foam (25 ppi) used in earlier studies of creation of negative Poisson's ratio foam [4, 5, 6]. This procedure resulted in completely different properties than those achieved in compressed

foams. Specifically, Poisson's ratios exceeding one were achieved. Moreover, substantial anisotropy in stiffness was generated.

2. Experimental procedure
2.1 Rationale
The Scott Industrial foam used in this study is a green polyurethane foam which has on average 65 pores per inch (ppi). From previous work, Scott foam of larger pore size [4] shows maximum re-entrant properties for final volumetric compression ratios of 3.3 to 3.7 [6]. Also, foam transformations at 170°C for 17 minutes gave rise to a minimum value of v (-0.7). These results, however, are based on a triaxial, mold compression procedure. In the present study, the Scott Industrial foam was placed under a uniaxial tension load and then, by heating and cooling, permanently deformed. Ultimately, it was desired to compare the mechanical properties (especially Poisson's ratio) of permanently stretched foam with triaxially compressed structures. In particular, it was anticipated that Poisson's ratio greater than 1/2 could be achieved.

2.2 Materials
The polyurethane foam [Scott Industrial foam, $\rho* = 0.03$ g/cm^3 (mass/volume), $\rho_s = 1.05 \sim 1.25$ g/cm^3 for solid polyurethane [8], l (length of cell rib) = 0.4 ± 0.03 mm] was obtained from Foamade Industries, Auburn Hills, MI, USA. The foam is reticulated with an open cell structure. The foam was provided in 2 meter lengths with a 5 cm × 5 cm square cross-section. This material was then cut into lengths for specimens. There was some variation in the relative density in each bar, however, the variation was considered negligible. The specimens were made geometrically similar so that changes in strain rate with time would be similar for all samples.

2.3 Specimen preparation
The foam samples were cut into bars with dimensions of 5 cm × 5 cm × 30 cm. Holes were punched through two opposite sides of the foam, 5 cm from each end. Two 0.5" (12.7 mm) diameter bars were pushed through these holes and mounted to a constant-strain jig. Dimensional measurements for Poisson's ratio, v, were taken for every 1 cm increment of axial displacement until the specimen failed. The oven was preheated to 30°C higher than the predetermined temperature (170°C) to compensate for a drop in temperature due to placement of the test jig. The samples were heated to a temperature in the range of 165°C ~ 175°C (via a mercury thermometer protruding from the oven top) for 17 minutes, as described in earlier studies of negative Poisson's ratio materials [4], [6]. The foam was then cooled to room temperature and the permanent strain was evaluated from dimensional measurements with a micrometer.

2.4 Scott foam test
Tensile tests were performed on the specimen with three settings of initial permanent strain: 0% (conventional or control), 25%, 35%, and 45%. Following procedures similar to those used in a prior study of conventional and re-entrant foam [6], the present foams were studied over a range of testing strains. For conventional Scott Industrial foam, Poisson's ratio increases rapidly under 25% ~ 45% tensile strain, with a maximum of $v = 0.55$ at $\varepsilon = 45\%$. Any further increase in strain results in a gradual decrease in Poisson's ratio from its peak value. It was decided to produce permanent transformation strain from 25% ~ 45%, since this region in the nonlinear behavior of conventional foam [6] produces a rapid change in Poisson's ratio with increasing strain. Three experiments with each strain value of foam were performed, the summarized data are plotted in the Results and Discussion section.

Fiduciary marks were made for displacement evaluation using a fine, indelible marker near the center of each specimen; the marks were made sufficiently far from the ends that the strain field would be uniform by virtue of Saint Venant's principle. These gauge lines were drawn in the middle of one side of the specimen; 4 cm apart in the longitudinal direction and 2 cm apart in the

transverse direction. Another set of lines for use in measuring both longitudinal and transverse strains was drawn on an adjacent face of the sample. Incremental differences in the spacing of the gauge lines were measured to calculate longitudinal and transverse strains to infer Poisson's ratio of the foam.

The top of each marked line was used as a reference point for measurement to minimize error. Although the measurements were taken with special care, the results showed errors at small strains. This can be attributed in part to the limiting resolution of one's eye (0.1 mm) in comparison with the size of the open cell structure of the foam specimen and the size of the ink marks. The calculated Poisson's ratio values had higher error for lower strain due to uncertainty in measured displacement; these errors were plotted as error bars in Fig. 1.

Engineering stress-strain curves were plotted from the load-displacement data. These tests were performed with the use of several dead weights suspended from the end of the specimen. The weights were converted to metric (N) and original cross-sectional area (A_0) was calculated from the bar dimensions. The strains (ε) in the direction of the applied load for each weight were plotted with stress ($P(N)/A_0$).

Both tensile and compression tests of all samples were performed to observe the mechanical behavior of the specimens. The modulus of elasticity of the material at small strains can be taken as the tangent modulus, E_t. In tensile tests, several data points were obtained for each sample's σ-ε curve. The tangent modulus, E_t, was taken between the origin and the first data point. The secant modulus, E_s, was found as the slope between the origin and the last data point. In compression tests, the final incremental load added to the column where buckling occurred was considered the critical buckling load. A 15-cm test section was cut from the middle of the sample, to avoid inhomogeneities caused by end effects. All of these columns were made geometrically similar, since the height of a column is inversely proportional to the square of the critical Euler buckling load.

In this study, the Young's modulus of each foam was already analyzed by virtue of its stress-strain curve. Also, the force causing catastrophic buckling to the column specimen was used to calculate the buckling strain in accordance with Hooke's law.

2.5 SEM evaluation of foams

The transformed and nontransformed Scott Industrial foams (polyurethane) were used in Scanning Electron Micrograph (SEM) evaluation ($\times$ 80). The transformed foams used in this analysis were subjected to a uniaxial tension as a result of permanent tensile strains of 25%, 35%, and 45% respectively. These pictures show the types of cell microstructure present in these foams. A Hitachi "Nature" SEM (Model No. S-2460N at Central Electron Microscopy Research Facility) was used for the study. The term "Nature" refers to a variable pressure inside the specimen chamber. An accelerating voltage of 3 keV was used to take micrographs of the samples which were sputter-coated with Au-Pd.

3. Results and Discussion

The Poisson's ratio versus engineering strain for the control and permanently stretched foam samples (for both sides) with 25%, 35%, and 45% strains are plotted in Fig. 1. Both adjacent sides of samples (Side A, Side B) show agreement with data points from Poisson's ratio measurements within the error bars. Therefore only data points from side A measurements were plotted in Fig. 1 to reduce the complexity of the figure. The control specimens exhibit a Poisson's ratio near 0.3 for lesser tensile strain and exceeds, then approaches, a value of 0.5 in tension, at large strain. A Poisson's ratio of greater than 0.5 does not violate any physical laws, but illustrates a possible anisotropic behavior due to the large strains causing alignment of cell ribs. The permanently deformed foam samples indicate similar behaviors, in which the Poisson's ratios were near 1.1 initially for small tension strains, then approached 0.6 for large tension strains. A maximum of Poisson's ratio was found to be at a strain value around 0.04. After this maximum, the Poisson's ratio of permanently deformed foam samples tended to converge on a value range of

0.5 ~ 0.8. Both specimen types (control and deformed) show a converging Poisson's ratio for strains larger than 25%. Tension tests of deformed samples were limited to smaller strains, since the foam was observed to tear near the supports for strain levels in the gauge section beyond 0.3.

Calculations for error bars in Fig. 1 were based on (i) the uncertainty in evaluating the distance between two marks, and (ii) the uncertainty from the limiting resolution of one's eye (0.1 mm). Where no error bars are visible, the uncertainty is smaller than the resolution of the graphic data point. The error bars are larger at smaller strain values because the differences in ε between original and deformed samples are small.

The Poisson's ratio in the transverse (perpendicular to the load used to create permanent axial deformation) direction was found to be large at high tensile engineering strains. Large strains were needed in these tests since the transverse specimens were small, so that displacement for a given strain was smaller than in the case of the larger longitudinal specimens. Transverse plane Poisson's ratio values were measured to be approximately 1.5 at $\varepsilon = 0.5$, in contrast to the Poisson's ratio of the control material: 0.5. The Poisson's ratio of the control material in the transverse plane was identical to the Poisson's ratio in longitudinal tests, confirming the isotropy of the unprocessed foam.

As for compression, the buckling strains exhibit decreasing values with increasing permanent strains. This behavior also can be explained by the reduction of resilience in samples processed at higher permanent strains. Actually it is simple. With processing, the stiffness increases due to cell rib alignment, but the collapse strength, governed by rib buckling, does not change much; consequently the strain associated with material buckling decreases with processing permanent strain.

Buckling in compression limited the measurements in compression since a measuring measurement of strain, needed to infer modulus and Poisson's ratio, can only be made under conditions of uniform strain in the gauge section. The buckling was an internal buckling (Fig. 2) rather than Euler column buckling. Buckling was observed even in very short specimens.

Band instability due to microbuckling has been seen previously in the plateau region of conventional foams [9]. Although those bands were of low contrast, presently observed specimen buckling is more macroscopic and more easily observable.

Engineering stress-strain curves for both longitudinal and transverse directions were evaluated from tensile tests of original and permanently stretched Scott Industrial foam samples. Resulting stress-strain curves for the axial (strained-tensional) direction are plotted in Fig. 3. Specimens with higher degrees of permanent strain, exhibited a higher stiffness and a lower strain value at failure. This phenomenon may be due to the fact that the highly stretched foam was already near the limitation of maximum strain for the foam material.

From the experimental stress-strain curve, the Young's modulus, E, was calculated via two graphical methods. The tangent modulus, E_t, is considered the slope of the line from the origin to the first data point. The secant modulus, E_s, was found as the slope of a line between the origin and a data point. For this comparison, the last data point in the series was used. These moduli are plotted in Fig. 4 versus permanent strain values. The longitudinal tangent modulus increased rapidly with the larger permanent strain values. These results, as inferred from the previous graph, show that the foam becomes stiffer in the axial (strained-tensional) direction by increasing the permanent strain value.

Fig. 5 shows the engineering stress-strain curves for tests measuring transverse sections of control and permanently stretched foams. As opposed to Fig. 3, stretched specimens with higher permanent strains show larger strain values at a given stress level. The transformed foam is anisotropic: it is much stiffer in the longitudinal direction than it is in the transverse direction.

Both secant and tangent moduli for the transverse direction were calculated from the data in the previous graph and displayed in Fig. 6. For a small strain range, data acquisition for tangent modulus was difficult due to a decrease of relative resolution. This problem was solved by using a "polynomial" function for curve fitting in the graphing software. Each stress-strain curve was considered as a quadratic function $\sigma = E_t \varepsilon + A \varepsilon^2$ and the value E_t from the curve-fit was used as

4

tangent modulus. Both mechanical moduli rapidly reduce with higher values of permanent strain in the foams. The transformed foam is considerably more compliant for tension in transverse directions than for the longitudinal direction (the direction of the permanent stretch).

Fig. 7 shows the micrograph of a control foam sample. The cells in this foam are rather round and symmetrical. It can be observed that cell ribs have a triangular cross-section. In comparison to the cellular structure in the control foam, the cells of the transformed foam are elongated and appear more irregular as shown in Fig. 8. In permanently stretched foam, cell ribs tend to align in one direction. Cell structures show sharp elliptical pores compared with the original foam. This type of combined deformation provides a reason for the small strain range observed in highly transformed specimens. Thus the SEM pictures confirm previous observations of mechanical anisotropy.

Foams which were transformed by permanent uniaxial stretching exhibited increased axial stiffness (by as much as a factor of 20), larger Poisson's ratio in excess of 1, and orientation of the microstructure. Poisson's ratios exceeding 1/2 are permissible in anisotropic materials. Indeed, hexagonal honeycombs can exhibit Poisson's ratio of 1, and if they have oriented hexagonal cells, greater than 1, in certain directions [2].

Materials with $v > \frac{1}{2}$ in both transverse directions have been termed "stretch densifying" in the terminology of Baughman [10], who found certain (anisotropic) crystals to exhibit such a property. The present foams exhibit a controllable stretch-densifying property, achieved by processing. The present anisotropic foams are in contrast to the re-entrant foams developed by one of the authors [4]; these foams were produced by triaxial permanent compression, and they exhibited reduced Young's modulus, negative Poisson's ratio, and a micro-buckling of the microstructure due to the processing.

4.   Conclusions

1.   The Poisson's ratio of samples with 25%, 35%, and 45% permanent uniaxial strains was about 1.1 at small tensile strain. These foams exhibited maximum values of Poisson's ratio around 1.5 at a strain of 0.04. At higher strain, the Poisson's ratio of both transformed and control foams tended to converge on a value range of 0.5 ~ 0.8.

2.   Compression experiments at small loads disclosed an internal banding form of buckling in permanently stretched foams.

3.   The transformed foam becomes stiffer in the axial (strained-tensional) direction, by a factor of up to 20.

4.   The values of secant and tangent modulus in the transverse direction of permanently stretched foams decrease with increasing permanent strain values. The transformed foam is considerably more compliant in tension, in transverse directions, than for longitudinal directions (the direction of the permanent stretch).

5.   SEM pictures of permanently stretched polyurethane shows elongated and irregular cell structure than control foams. This deformation characteristic accounts for the anisotropy observed in highly transformed specimens.

References
1.   M. F. Ashby, The Mechanical properties of cellular solids, Metallurgical Transactions A, Vol. 14A, pp. 1755-1769, 1983
2.   L. J. Gibson, M. F. Ashby, Cellular solids, Pergamon Press, Oxford, 1988
3.   Y. C. Fung, Foundation of Solid Mechanics, Prentice-Hall, Englewood Cliffs, NJ,   1968
4.   R. S. Lakes, Foam structures with a negative Poisson's ratio, Science, Vol. 235,   pp. 1038-1040, 1987

5

5. E. A. Friis, R. S. Lakes, J. B. Park, Negative Poisson's ratio polymeric and metallic foams, J. Mat. Sci., Vol. 23, pp. 4406-4414, 1988
6. J. B. Choi, R. S. Lakes, Non-linear properties of polymer cellular materials with a negative Poisson's ratio, J. Mat. Sci., Vol. 27, pp. 4678-4684, 1992
7. J. B. Choi, R. S. Lakes, Non-linear properties of metallic cellular materials with a negative Poisson's ratio, J. Mat. Sci., Vol. 27, pp. 5375-5381, 1992
8. Modern Plastics Encyclopedia, Vol. 51, No. 10A, 1974-1975
9. R. Lakes, P. Rosakis, A. Ruina, Microbuckling instability in elastomeric cellular solids, J. Mat. Sci., Vol. 28, pp. 4667-4672, 1993
10. R. H. Baughman, D. S. Galvao, Crystalline networks with unusual predicted mechanical and thermal properties, Nature, Vol. 365, pp. 735-737, 1993
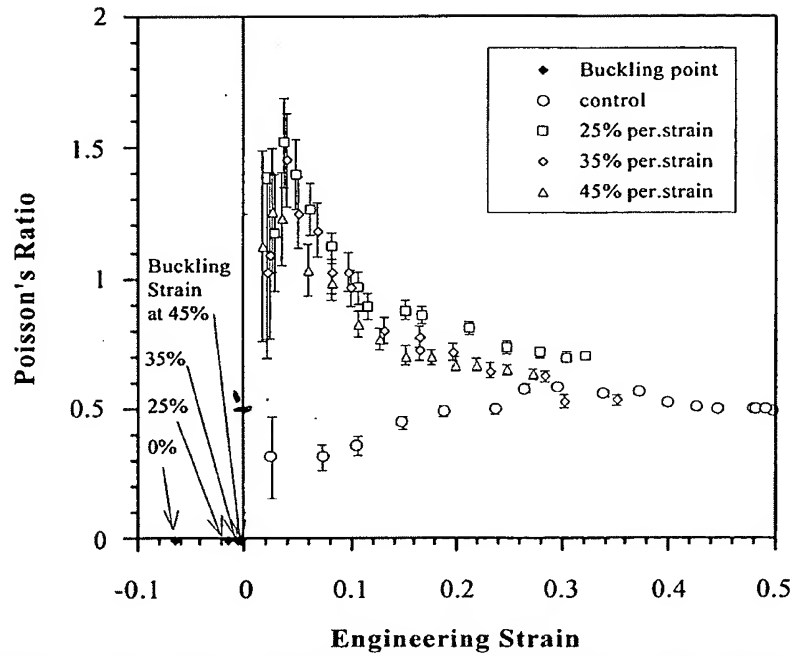
Figures

Figure 1 Poisson's ratio versus engineering strain for original and permanently stretched Scott Industrial foam samples; solid diamond represents internal buckling strain; Poisson's ratio not measured. Circles, squares, diamonds and triangles represent control, permanent strain values of 25%, 35%, and 45%, respectively.

Figure 2 Demonstration of the buckling in the permanently stretched Scott foam under compression
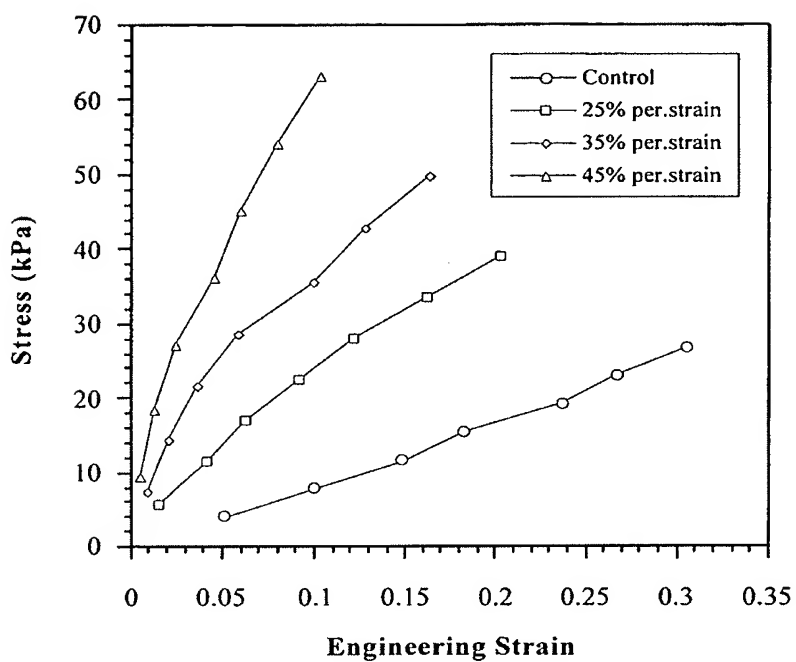
Figure 3 Engineering stress versus strain curve for original and permanently stretched Scott foam samples in longitudinal direction. Circles, squares, diamonds and triangles represent control, permanent strain values of 25%, 35%, and 45%, respectively.
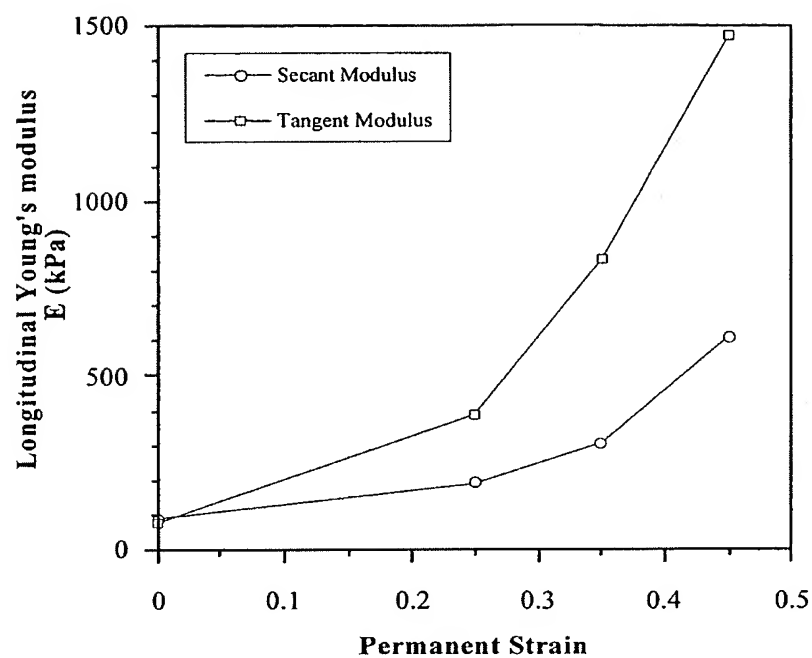
Figure 4 Longitudinal Young's modulus versus permanent strain for original and permanently stretched Scott foam samples. Circles and squares represent secant and tangent modulus, respectively.

Figure 5 Engineering stress versus strain curve for original and permanently stretched Scott foam samples in transverse direction. Circles, squares, diamonds and triangles represent control, permanent strain values of 25%, 35%, and 45%, respectively.

Figure 6 Transverse Young's modulus versus permanent strain for original and permanently stretched Scott foam samples. Circles and squares represent secant and tangent modulus, respectively.
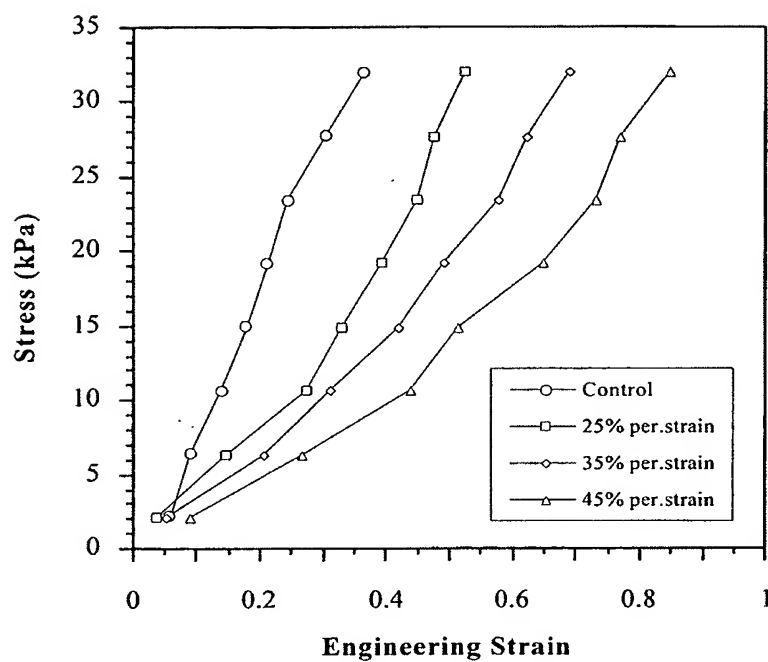
Figure 7 Scanning electron micrograph of conventional Scott Industrial foam. Magnification × 80, accelerating voltage 3 keV.

Figure 8 Scanning electron micrograph of 45% permanently stretched Scott Industrial foam. Magnification × 80, accelerating voltage 3 keV.

Figure 1 Poisson's ratio versus engineering strain for original and permanently stretched Scott Industrial foam samples; solid diamond represents internal buckling strain; Poisson's ratio not measured. Circles, squares, diamonds and triangles represent control, permanent strain values of 25%, 35%, and 45%, respectively.

Figure 2 Demonstration of the buckling in the permanently stretched Scott foam under compression

Figure 3 Engineering stress versus strain curve for original (control: zero permanent strain) and permanently stretched Scott foam samples in longitudinal direction. Circles, squares, diamonds and triangles represent control, permanent strain values of 25%, 35%, and 45%, respectively.
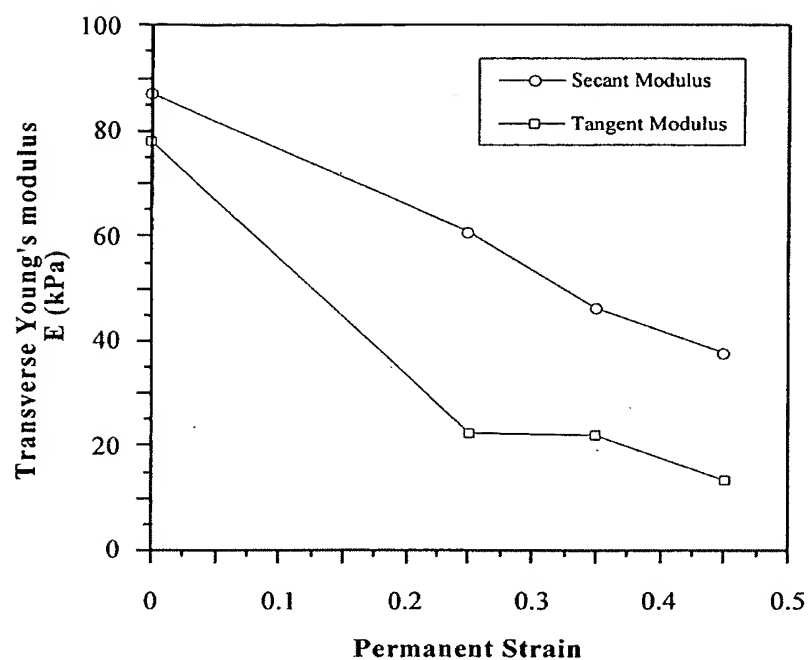
8

Figure 4   Longitudinal Young's modulus versus permanent strain for original (control: zero permanent strain) and permanently stretched Scott foam samples. Circles and squares represent secant and tangent modulus, respectively.

Figure 5 Engineering stress versus strain curve for original (control: zero permanent strain) and permanently stretched Scott foam samples in transverse direction. Circles, squares, diamonds and triangles represent control, permanent strain values of 25%, 35%, and 45%, respectively.

Figure 6 Transverse Young's modulus versus permanent strain for original (control: zero permanent strain) and permanently stretched Scott foam samples. Circles and squares represent secant and tangent modulus, respectively.

Figure 7 Scanning electron micrograph of conventional Scott Industrial foam. Magnification × 80, accelerating voltage 3 keV.

Figure 8 Scanning electron micrograph of 45% permanently stretched Scott Industrial foam. Magnification × 80, accelerating voltage 3 keV.

EXHIBIT B
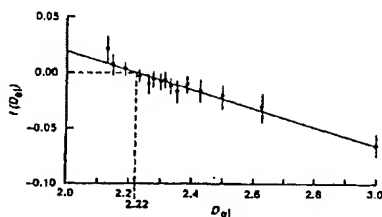
Fig. 4. The function $f(D_{el})$ as described in the text is the average of data taken from 20 scans, and is based on 15 different values of D_{el} and 9 reflectivity thresholds (for a total of $9 \times 15 \times 20 = 2700$ dimensions). Averages and standard deviations, indicated by the error bars, are plotted. The least-squares linear regression is shown and has a horizontal intercept $(D_{el} = d_{el})$ of 2.22.

Furthermore, the above formula for $C_{D_a}(T_i)$ shows that

$$f(D_{el}) = (D_{el}/d_{el} - 1)\sum_{i=1}^{k} C_2(T_i) \qquad (4)$$

Hence $f(D_{el})$ is linear.

Figure 4 shows the result as D_{el} is varied through 15 values between 3.0 and 2.13; the latter was the lowest value accessible with the data set [this corresponded to boxes of 1 by 1 by 1 pixel and boxes 190 by 190 by 2 pixels (twice the anisotropic scale), where $2.13 = 2 + \log 2/\log 190$]. The same nine thresholds were used as before. The function $f(D_{el})$ was determined separately on 20 radar rain fields; the linear regression shown yields $d_{el} = 2.22 \pm 0.07$. The error is the standard deviation of d_{el} estimated from each of the 20 scans separately. These scans were chosen at random from data from the Montreal region during summer of 1984, all on separate days. The individual slopes and axis intercepts varied by ± 11 and ± 9 percent, respectively, which indicated that any systematic variation is small.

An obvious application of this result is to quantitatively measure the stratification. For example, the rain field is considerably more stratified than the wind field, which has a value $d_{el} = 23/9 = 2.555 \ldots$ that has been estimated from energy spectra and dimensional arguments (6). These elliptical dimensions are necessary in both additive (8) and multiplicative [cascade-type (7, 9, 10, 22, 23)] stochastic mesoscale modeling (16). In numerical weather prediction models, the calculated and empirical values of d_{el} can be compared to study the "stochastic coherence" (24) of the calculated values. When fields are stratified, efficient modeling and measurement procedures must involve choosing discrete vertical and horizontal scales that are "comparable"; the elliptical dimension gives us the required exponent. This poses interesting theoretical questions for dynamical models that involve interacting fields with different degrees of stratification.

REFERENCES AND NOTES

1. S. Lovejoy, *Science* 216, 185 (1982).
2. D. Schertzer and S. Lovejoy, in *Proceedings of the Fourth Symposium on Turbulent Shear Flows* (University of Karlsruhe, West Germany, 1983), p. 11.18.
3. S. Lovejoy and D. Schertzer, in *Preprints, Sixth Symposium on Turbulence and Diffusion* (American Meteorological Society, Boston, 1983), p. 102; D. Schertzer and S. Lovejoy, in *Preprints, Fourth Conference on Atmospheric and Oceanic Waves and Stability* (American Meteorological Society, Boston, 1983), p. 58.
4. D. Schertzer and S. Lovejoy, in *Preprints, International Union of Theoretical and Applied Mechanics Symposium on Turbulence and Chaotic Phenomena in Fluids* (International Union of Theoretical and Applied Mechanics, Kyoto, Japan, 5 to 10 September 1983) p. 141.
5. ———, *Turbulence and Chaotic Phenomena in Fluids*, T. Tatsumi, Ed. (North-Holland, Amsterdam, 1984), p. 505.
6. ———, in *Turbulent Shear Flow*, L. J. Bradbury and F. Durst, Eds. (Springer, New York, 1985), vol. 4, pp. 7–33.
7. ———, *Phys. Chem. Hydrodyn.* 6, 623 (1985).
8. S. Lovejoy and D. Schertzer, *Water Resour. Res.* 21, 1233 (1985).
9. D. Schertzer and S. Lovejoy, *Fractals in Physics*, S. Pietronero and E. Tosatti, Eds. (North-Holland, Amsterdam, 1986), p. 457.
10. ———, *J. Geophys. Res.*, in press.
11. H. G. E. Hentschel and I. Proccacia, *Physica* 8D, 435 (1983).
12. P. Grassberger, *Phys. Lett.* 97A, 227 (1983).
13. U. Frisch and G. Parisi, in *Turbulence and Predictability in Geophysical Fluid Dynamics and Climate Dynamics*, M. Ghil, R. Benzi, G. Parisi, Eds.

(North-Holland, Amsterdam, 1985), p. 84.
14. T. C. Halsey, M. H. Jensen, L. P. Kadanoff, I. Proccacia, B. I. Shraiman, *Phys. Rev. A* 33, 1141 (1986).
15. S. Lovejoy and D. Schertzer, *Digital Image Processing in Remote Sensing*, J. P. Muller, Ed. (Francis and Taylor, London, in press), chap. 14.
16. ———, *Bull. Am. Meteorol. Soc.* 67, 21 (1986).
17. ———, P. Ladoy, *Nature (London)* 319, 43 (1986).
18. ———, *ibid.* 320, 401 (1986).
19. P. Gabriel, S. Lovejoy, G. L. Austin, D. Schertzer, in *Preprints, Sixth Conference on Atmospheric Radiation* (American Meteorological Society, Boston, 1986), p. 230.
20. The standard error of the fits was computed. The maximum value for all the fits (the largest T was used) was ± 0.07.
21. B. Kerman, K. Szeto, S. Lovejoy, D. Schertzer, in *Preprints, Nonlinear Variability in Geophysics* (McGill University, Montreal, 1986), p. 34.
22. D. Schertzer and S. Lovejoy, *Ann. Math. Quebec* in press.
23. Multiplicative processes are required if we are to obtain the necessary hierarchy of fractal dimensions.
24. D. Schertzer et al., in *Preprints, International Association of Meteorology and Atmospheric Physics and the World Meteorological Organization Symposium on the Maintenance of the Quasi-Stationary Components of the Flow in the Atmosphere and in Atmospheric Models*, (World Meteorological Organization, Geneva, 1983), p. 325.
25. We acknowledge discussions with G. L. Austin, P. Gabriel, V. K. Gupta, J. P. Kahane, P. Ladoy, D. Lavallée, E. Levitch, J. P. Muller, R. Peschanski, A. Saucier, T. Warn, E. Waymire, and J. Wilson. We thank the Aspen Center for Physics for their hospitality.

23 September 1986; accepted 6 January 1987

Foam Structures with a Negative Poisson's Ratio

Roderic Lakes

A novel foam structure is presented, which exhibits a negative Poisson's ratio. Such a material expands laterally when stretched, in contrast to ordinary materials.

VIRTUALLY ALL COMMON MATERIALS undergo a transverse contraction when stretched in one direction and a transverse expansion when compressed. The magnitude of this transverse deformation is governed by a material property known as Poisson's ratio. Poisson's ratio is defined as the negative transverse strain divided by the axial strain in the direction of stretching force. Since ordinary materials contract laterally when stretched and expand laterally when compressed, Poisson's ratio for such materials is positive. Poisson's ratios for various materials are approximately 0.5 for rubbers and soft biological tissues, 0.45 for lead, 0.33 for aluminum, 0.27 for common steels, 0.1 to 0.4 for typical polymer foams, and nearly zero for cork.

Negative Poisson's ratios are theoretically permissible but have not, with few exceptions, been observed in real materials. Specifically, in an isotropic material (a material that does not have a preferred orientation) the allowable range of Poisson's ratio is from -1.0 to $+0.5$, based on thermodynamic considerations of strain energy in the

theory of elasticity (1). It is believed by many that materials with negative values of Poisson's ratio are unknown (1); however, Love (2) presented a single example of cubic "single crystal" pyrite with a Poisson's ratio of -0.14 and he suggested that the effect may result from a twinned crystal. Analysis of the tensorial elastic constants of anisotropic single crystal cadmium suggests that Poisson's ratio may attain negative values in some directions (3). Anisotropic, macroscopic two-dimensional flexible models of certain honeycomb structures (not materials) have exhibited negative Poisson's ratios in some directions (4). These known examples of negative Poisson's ratios all depend on the presence of a high degree of anisotropy; the effect only occurs in some directions and may be dominated by coupling between stretching force and shear deformation. The materials described in this report, by contrast, need not be anisotropic.

Foams with negative Poisson's ratios were

Department of Biomedical Engineering, University of Iowa, Iowa City, IA 52242.

produced from conventional low-density open-cell polymer foams (Fig. 1) by causing the ribs of each cell to permanently protrude inward; this resulted in a reentrant structure such as that shown in Fig. 2. An idealized reentrant unit cell is shown in Fig. 3. A polyester foam (5) was used as a starting material and was found to have a density of 0.03 g cm^{-3}, a Young's modulus of 71 kPa, a cell size of 1.2 mm, and a Poisson's ratio of 0.4. The method used to create the reentrant structure is as follows. Specimens of conventional foam were compressed triaxially, that is, in three orthogonal directions, and were placed in a mold. The mold was heated to a temperature slightly above the softening temperature of the foam material, 163° to 171°C in this case. The mold was then

cooled to room temperature and the foam was extracted. Specimens that were given a permanent volumetric compression factor of between 1.4 and 4 during this transformation were found to exhibit negative Poisson's ratios. For example, a foam subjected to a permanent volumetric compression factor of 2 had a Young's modulus of 72 kPa, and a Poisson's ratio of −0.7. Polyester foams of similar structure and properties, but different cell sizes (0.3, 0.4, and 2.5 mm), transformed by the above procedure were also found to exhibit negative Poisson's ratios. Reticulated metal foams were transformed by the alternate procedure of plastically deforming the material at room temperature. Permanent compressions were performed sequentially in each of three or-
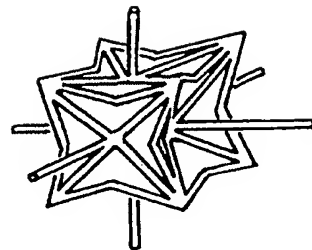

Fig. 3. Idealized reentrant unit cell produced by symmetrical collapse of a 24-sided polyhedron with cubic symmetry.

thogonal directions. Foams transformed in this way were also found to exhibit reentrant structures.

The casual observer may comment that materials with negative Poisson's ratios are counterintuitive in that they do not conserve volume. This is not objectionable since there is no law of conservation of volume. Various observers develop insights about these physical properties from rubbery materials that are indeed nearly incompressible. Nevertheless, such common materials such as steel, aluminum, conventional foams, and hard plastics have Poisson's ratios that differ from 0.5, hence these materials do not conserve volume. All known materials, including the ones described here, obey conservation of energy, which restricts Poisson's ratio to be between −1.0 and 0.5 for isotropic materials. The physical origin of the negative Poisson's ratio can be appreciated in view of the idealized unit cell shown in Fig. 3. Tension applied to the vertical links will cause the cell to unfold and expand laterally. The actual cell structure (Fig. 2) also contains ribs which are bent and protrude into the cells.

Foams with negative Poisson's ratios were found to be more resilient than conventional foams. Foams with a typical structure of tetrakaidecahedral (14-sided) cells (6) exhibit an approximately linear compressive stress-strain curve up to about 5% strain (7). At higher strains, the cell ribs buckle and the foam collapses at constant stress. Reentrant foams exhibited a nearly linear relation between stress and strain up to more than 40% strain, with no abrupt collapse. Resilience was enhanced for deformation in each of three orthogonal directions. Improved resilience (in one direction) has also been reported in foams compressed permanently in one direction (uniaxially) (8). I prepared such foams and found that they exhibited Poisson's ratios near zero. They did not exhibit negative values.

It is notable that the theory of elasticity contains no characteristic length scale. The
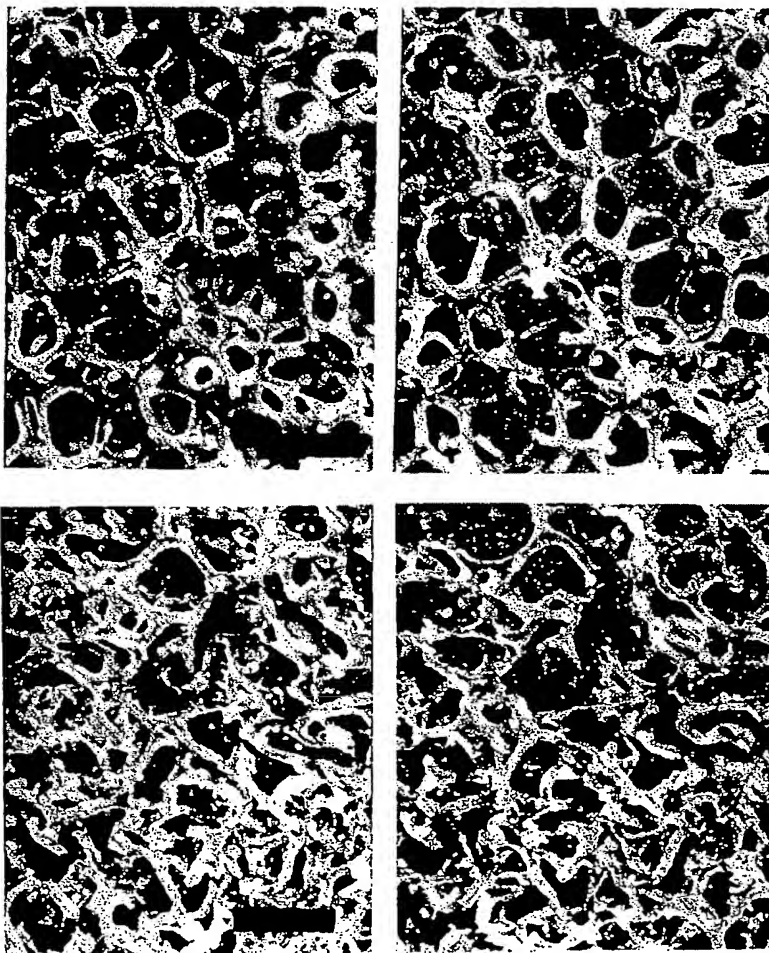

Fig. 1 (top). Stereo photograph of a conventional open-cell polymer foam. Scale mark, 2 mm. **Fig. 2 (bottom).** Stereo photograph of a reentrant foam. Permanent volumetric compression factor is 2.7. Poisson's ratio is −0.6. Scale mark, 2 mm.

phenomenon of a negative Poisson's ratio consequently does not require a coarse cellular structure or depend on the structure size. In principle, materials with microstructure on a scale smaller than 1 μm could exhibit a negative Poisson's ratio. The theory of elasticity also predicts a variety of unusual phenomena to occur in solids with a negative Poisson's ratio. For example, the top and bottom lateral surfaces of a bent prismatic beam of a conventional material with a positive Poisson's ratio assume a saddle shape: the "anticlastic curvature" of bending, in which the transverse curvature is opposite the principal curvature of bending (9). In the case of a negative Poisson's ratio, the theory of elasticity predicts that these surfaces will assume an ellipsoidal shape, or a synclastic curvature. I have observed such synclastic curvature in bent bars of transformed foam. Furthermore, in the indentation of a block of material caused by a localized pressure distribution, the indentation for a given pressure is proportional to $(1 - v^2)/E$, in which E is Young's modulus and v is Poisson's ratio. Consequently, a material with a negative Poisson's ratio approaching the thermodynamic limit $v = -1.0$ will be difficult to indent even if the material is compliant. The origin of this predicted phenomenon may be traced to the relation between the shear modulus G, the bulk modulus B (the inverse of the compressibility), and Poisson's ratio v: $B = 2G(1 + v)/(1 - 2v)$. When the Poisson's ratio approaches 0.5, as in rubbery solids, the bulk modulus greatly exceeds the shear modulus and the material is referred to as incompressible. When Poisson's ratio approaches -1.0, the material becomes highly compressible; its bulk modulus is much less than its shear modulus. The toughness of a material can also depend on its Poisson's ratio. Specifically, the critical tensile stress (10) for fracture of a solid of surface tension T, Young's modulus E, with a plane circular crack of radius r is $[\pi ET/2r(1 - v^2)]^{1/2}$. When the Poisson's ratio approaches -1.0, the material is predicted to become very tough.

Applications of novel, reentrant foams with negative Poisson's ratios may be envisaged in view of these properties. An example of the practical application of a particular value of Poisson's ratio is the cork of a wine bottle. The cork must be easily inserted and removed, yet it also must withstand the pressure from within the bottle. Rubber, with a Poisson's ratio of 0.5, could not be used for this purpose because it would expand when compressed into the neck of the bottle and would jam. Cork, by contrast, with a Poisson's ratio of nearly zero, is ideal in this application. It is anticipated that

reentrant foams may be used in such applications as sponges, robust shock-absorbing material, air filters, and fasteners.

REFERENCES AND NOTES

1. Y. C. Fung, *Foundations of Solid Mechanics* (Prentice-Hall, Englewood Cliffs, NJ, 1968), p. 353.
2. A. E. H. Love, *A Treatise on the Mathematical Theory of Elasticity* (Dover, New York, ed. 4, 1944).
3. Y. Li, *Phys. Status Solidi* 38, 171 (1976).
4. L. J. Gibson, M. F. Ashby, G. S. Schajer, C. I. Robertson, *Proc. R. Soc. London A* 382, 25 (1982).
5. Scott Industrial Foam, Scott Paper Company.
6. H. A. Lanceley, J. Mann, G. Pogany, in *Composite Materials*, L. Holliday, Ed. (Elsevier, New York, 1966), chap. 6.
7. M. F. Ashby, *Metall. Trans.* 14A, 1755 (1983).
8. W. R. Powers, U.S. Patent 3 025 200 (1962).
9. S. P. Timoshenko and J. N. Goodier, *Theory of Elasticity* (McGraw-Hill, New York, ed. 3, 1982).
10. I. N. Sneddon, *Fourier Transforms* (McGraw-Hill, New York, 1951).
11. I thank the University of Iowa Research Foundation for filing a patent application for this invention. Specimens of polyester foam were kindly supplied by Foamade Industries, Auburn Hills, MI.

Encystation and Expression of Cyst Antigens by Giardia lamblia in Vitro

FRANCES D. GILLIN, DAVID S. REINER, MICHAEL J. GAULT, HERNDON DOUGLAS, SIDDHARTHA DAS, ANNETTE WUNDERLICH, JUDITH F. SAUCH

The cyst form of *Giardia lamblia* is responsible for transmission of giardiasis, a common waterborne intestinal disease. In these studies, encystation of *Giardia lamblia* in vitro was demonstrated by morphologic, immunologic, and biochemical criteria. In the suckling mouse model, the jejunum was shown to be a major site of encystation of the parasite. Small intestinal factors were therefore tested as stimuli of encystation. An antiserum that reacted with cysts, but not with cultured trophozoites was raised in rabbits and used as a sensitive probe for differentiation in vitro. Cultured trophozoites that were exposed to bile salts showed a more than 20-fold increase in the number of oval, refractile cells that reacted strongly with anticyst antibodies, and in the expression of major cyst antigens. Exposure to primary bile salts resulted in higher levels of encystation than exposure to secondary bile salts. These studies will aid in understanding the differentiation of an important protozoan pathogen.

GIARDIASIS, A MAJOR HUMAN INtestinal disease worldwide, is transmitted by ingestion of the oval cyst form of *Giardia lamblia* from fecally contaminated water or food (1). Exposure of cysts to gastric acid triggers excystation in the duodenum (2). Emerging flagellated trophozoites divide and colonize the small intestine where some remain and cause diarrhea, while others encyst and are passed in feces, completing the life cycle (3). Although trophozoites can be cultured in vitro (4), neither encystation nor expression of cyst antigens in vitro has been reported. The studies presented here were designed to (i) elucidate the process of encystation in vivo; (ii) develop sensitive reagents for the detection and quantitation of differentiation in vitro; and (iii) develop a system for induction of encystation of trophozoites cultured in vitro.

Since little is known about encystation of *G. lamblia*, we studied the location of cysts and trophozoites along the small and large intestine of suckling mice as a function of time after infection. Three-day-old suckling mice (strain CF1) were infected (5) with 10^3 axenically cultured *G. lamblia* trophozoites

by direct transcutaneous injection into the milk-filled stomach (6). Trophozoites of strain WB (ATCC #30957) had been grown to late log phase in supplemented (6) Diamond's TYI-S-33 medium (7) as described (8), washed, and resuspended in 0.2 ml of 0.1M phosphate-buffered saline (PBS; pH 7.2). We found cysts in every intestinal section, although few were in the duodenal section "D" (Fig. 1). Through day 16, large numbers of cysts were in sections 3 or 4 (mid to lower jejunum). As infection progressed, increasing proportions of cysts were found in the large intestine. Since cysts are not motile and therefore move downstream with the flow of intestinal fluid, sections 3 and 4 appeared to be major sites of encystation. The percentage of parasites in cyst form per mouse averaged 8.6 (from nine determinations, days 4 through 20, range,

F. D. Gillin, D. S. Reiner, M. J. Gault, S. Das, Department of Pathology, University of California, San Diego Medical Center H811F, San Diego, CA 92103.
A. Wunderlich and H. Douglas, Department of Medicine, University of California, San Diego Medical Center H811F, San Diego, CA 92103.
J. F. Sauch, Health Effects Research Laboratory, U.S. Environmental Protection Agency, Cincinnati, OH 45268.

EXHIBIT C

PASSIVE AND MR-FLUID COATED AUXETIC FOAM – MECHANICAL AND ELECTROMAGNETIC PROPERTIES

F. Scarpa[a], F.C. Smith[b] and A. Cannas[a]

[a] *Multidomain Cellular Solids Laboratory, Department of Mechanical Engineering, University of Sheffield, Sheffield S1 3JD, e-mail: f.scarpa@shef.ac.uk*
[b] *Department of Engineering, University of Hull – Kingston upon Hull, HU6 7RX, UK, e-mail: f.c.smith@hull.ac.uk*

SOMMARIO

Nel presente articolo vengono esaminate alcune proprietá meccaniche e dielettriche di schiume poliuretaniche auxetiche con e senza ricoprimento superficiale a base di fluido magnetoreologico (MR). Le schiume auxetiche mostrano capacita' di ricovero a carichi dinamici (crash) superiori alla schiuma convenzionale di base. Le proprieta' dielettriche, in particolare i fattori di perdita nel campo delle frequenze sono incrementati dalla presenza di un ricoprimento a base di liquido magnetoreologico.

ABSTRACT

The following paper shows a comparative study on the mechanical and dielectric properties of a novel class of auxetic (negative Poisson's ratio) rigid polyurethane foam. An auxetic solid expands in all directions when pulled in only one, thus behaving in an opposite manner compared to "classical" solids. The auxetic PU foam considered shows enhanced crashworthiness properties, and nonlinear elastic restoring force capabilities. Samples of auxetic foam coated with MR fluid allow also a substantial increase in dielectric loss factors when compared to conventional foams.

1. INTRODUCTION

Since 1987, when isotropic auxetic foam was manufactured for the first time [1], negative Poisson's ratio materials have created some interest for potential applications in various fields, such as structural integrity compliant structures and sandwich components [2]. By definition, an auxetic (or negative Poisson's ratio) material expands in all directions when pulled in only one, giving therefore a deformation kinematics opposite to the one of "conventional" materials. A negative Poisson's ratio coefficient for a material could lead, for example, to an increase in indentation resistance [3], enhanced bending stiffness and shear resistance in structural elements [4-5] and optimal passive tuning of structural vibrations [6].

Applications exist for materials that exhibit simultaneously enhanced performance in the structural and electromagnetic domains. An electromagnetic analogue of an 'auxetic characteristic does not exist, and a beneficial auxetic behaviour is not necessarily accompanied by improved performance in the electromagnetic domain. However, the authors have shown that auxetic materials exhibit a wide range of electromagnetic properties, and these can affect better designs in the electromagnetic domain [7,8]. An important engineering application that requires enhanced structural and electromagnetic performance is shielding, where a mechanically protective structure is also required to absorb or reflect electromagnetic waves.

Foam materials are widespread used for packaging solutions and applications like automotive trimming, seat cushion, acoustic insulation [1, 13]. They constitute also a core base material for Salisbury screens or EM wave absorber structure [7, 8]. The dimensionless quantity relative permittivity (written as ε_r) is the electromagnetic parameter that dictates the electrical characteristics of a material. It is a measure of the polarizability of a material and can be a real, complex or tensor quantity. Relative permeability (μ_r) is the equivalent quantity for magnetic fields. When an electromagnetic wave is incident upon a boundary where there is a change in the ratio μ_r / ε_r reflections occur and some of the energy present in the incident wave is not transmitted through the boundary. Furthermore, if either ε_r or μ_r are complex, energy in this region will be absorbed and dissipated as heat. To construct an absorbing or reflecting shield, it is therefore necessary to control the complex permittivity and/or permeability of the shielding material. Conventional foams are not efficient absorbers or reflectors; this is because their electromagnetic properties do not differ markedly from those of free space (due to the low material volume fraction of foams and the low relative permittivity and permeability of the base materials). However, treated auxetic foams can exhibit a higher effective permittivity and permeability, which potentially opens up new applications related to shielding and packaging.

Auxetic open cell polymeric foams show significant strain dependence over the Poisson's ratio [9], and enhanced resilience under compression, with a nearly linear relationship up to 40 % strain [1]. The same improvement in resilience can be found also in foam under permanent uniaxial compression [10], although they do not show a negative Poisson's ratio behaviour. In this paper is described a type of negative Poisson's ratio PU foam exhibiting some characteristic features of polymeric auxetic foams published in open literature: enhanced resilience under compression, strain dependence of the Poisson's ratio, with a significant resilience under high constant strain loading. In fact, while the conventional grey PU foam used for manufacture of the auxetic foam did not show any particular resilience under such loading (up to $54s^{-1}$ on samples with a length of 0.04 m), the auxetic foam indicated a stress-strain relation characteristic of high density polyurethane foams [11].

The paper describes the set of mechanical and electromagnetic tests performed to measure the Poisson's ratio under uniaxial tension loading, static compression, tension characteristics, magnetic permittivity and dielectric loss factor of the conventional and auxetic foam. The high constant strain rate (dynamic crush loading) of the foams has been performed using a cam plastometer capable of maximum strain rates of 200 s^{-1}, and especially designed to test polymeric foams. The results have been then postprocessed using the Nagy rheological law [14] for high constant strain rate loading for future implementations in crashworthiness simulations codes. Mechanical tensile and EM tests have also been performed on samples of auxetic foam coated with MR fluid. MR fluids are composed by dispersions of metal (iron) particulate in a solution composed typically by silicon or mineral oil. The response of MR fluid results fro the polarisation of suspended particles by application of external magnetic field, giving rise to an increase in viscosity of the whole solution [17]. In the context of this paper, the MR fluid has been used as a coating medium to provide interaction between inserts (carbonyl particles) and the struts of the foam unit cells under external field.

2. MECHANICAL PROPERTIES
The auxetic foam specimens were manufactured from open cell polyurethane foam supplied by McMaster-Carr Co., Chicago, IL. The density of the foam was 32 kg m^{-3}. The foam was cut into circular specimens, inserted in a mould made from aluminium tubes and put inside a

constant temperature oven, following a manufacturing route described in [12]. The auxetic specimens had a final diameter of 0.019 m, with a length of 0.040 m.

A magnetorheological fluid (Lord MF132) was used to coat some auxetic samples. The fluid is composed by iron carbonyl particles with average diameter of 5μm embedded in a silicon oil solution. The coating was performed putting the samples in a tray filled with MR fluid, and letting a constant roll of the specimens in order to obtain a uniform coating distribution on the external surface. The samples were then left to expel the excess of fluid for 48 hours.

2.1 Testing methods

The Poisson's ratio of the auxetic foams was measured using an Image Data Detection technique applied to pictures of the foam specimens collected under tensile loading using a high quality digital camera. The outer edges of auxetic foam sample were connected in the longitudinal direction to the internal surface of a clamp using epoxy glue, and different tensile engineering strains (up to 135%) were applied. After each loading, the specimen was returned to the initial undeformed position. For each applied strain, images were taken in the loaded and unloaded states. The edges of the specimen were detected from the images using Mallat's wavelet image detection method [12] implemented in the MATLAB programming environment. All edge measurements were taken in pixels, and the lengths measured excluded the epoxy glue parts of the foam, so that the Saint Venant effects due to the clamp boundaries were avoided. The tests were carried out at a temperature of 19° Celsius.

The static uniaxial tension and compression tests were performed on the conventional and auxetic foams using a Hounsfield Tensometer. The foam samples were connected to clamps with epoxy glue, and the load applied with steps of 2.5 N on average. The maximum load applied during the tensile tests in tension was 40 N (both for the conventional and auxetic foam). In the case of the compression tests, the maximum load for the different samples was 50 N. Measurements were taken at intervals of 20 sec, to avoid hysteresis during the recovery period of the samples. All tests we carried at a temperature of 18° Celsius.

The dynamic crash loading tests were performed using a cam plastometer [12] developed for constant high strain rate tests with large displacements. The profile of the cam dictates the displacement-time relationship during loading. The cam plastometer used in these experiments is capable of conducting tests at constant true strain or constant engineering strain at rates up to 200 s^{-1} and displacement up to 50 mm. For the tests a cam were used to provide displacements of 50 mm at a constant cross-head velocities, which generated constant engineering strain rate loading of the sample. Selecting different gears in the transmission between the driving motor and the loading cam varied the strain rate. The eight 40 mm long, 19 mm diameter specimens were packed together to form a quasi circular cross section of 80 mm diameter. The tests were conducted using three constant engineering strain rates of 54s^{-1}, 38s^{-1} and 15 s^{-1}, equivalent respectively to velocities of 5.4, 3.8 and 1.5 m s^{-1}. The signals related to the reaction forces and displacement histories were detected using a NovaTech 10 kN load cell and a purpose made capacitive displacement transducer respectively. The output signals were collected using a LabView program through a NI DataTranslation 3005 multifunctional I/O board in an Intel based PC. The signals were sampled at a frequency of 350 Hz. The same test procedure was also carried out on a similar package of normal open cell polyurethane foam to perform a comparison between the positive and negative Poisson's ratio cellular solids. All test were performed at a temperature of 18° Celsius and relative humidity around 45 %. The auxetic foam samples with MR fluid coating were tested at the same environmental conditions under quasistatic tensile test only.

2.2 Results

Figure 1 shows the behaviour of the Poisson's ratio versus the tensile engineering strain. One can observe that the measured Poisson's ratio mean value is approaching –0.04 for tensile strains between 60 % and 117 %. After those values, the Poisson's ratio of the specimen increases for increasing tensile loading, in a similar manner to other auxetic foams tested in literature. Compared to other auxetics foams [4, 9], the measured values of the Poisson's ratio are, at least, one order of magnitude lower. Although small, the auxetic effect of the specimens was noticeable, particularly considering the fact that the original open cell polyurethane foam had a density around 30-35 pores per inch.
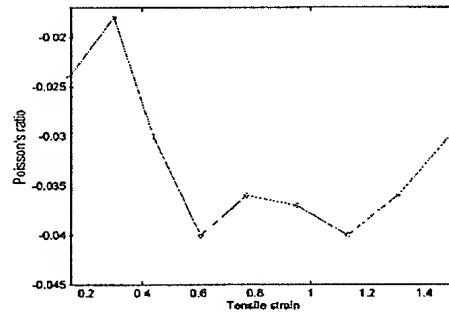
Fig 1. Strain dependence of the Poisson's ratio under tensile test.

Figure 2 shows the static tensile tests results carried out on the conventional and auxetic foam samples. The conventional grey rigid PU foam behaves in compression and tension like a typical elastic-plastic foam [13]. In compression, the linear elastic part of the stress-strain curves shows a Young's modulus of 470 kPa, and a plastic yielding stress of 46 kPa. The densification effects become important after engineering strains higher than 60 %. In tension, the linear elasticity part of the curve gives a Young's modulus of 780 kPa, with a plastic yield of 45 kPa, and a failure stress of 93 kPa at 35 % of elongation. The auxetic PU foam has a peculiar behaviour, in particular for tension loading. The linear elastic part of the stress-strain curve indicates a Young's modulus of 1 MPa. The yield stress of 62 kPA occurs at a strain of 2.2 %. After that value, the plateau region of the curve extends to strains up to 120 %. This fact is explained by the unfolding of the convolute cell ribs under pure tensile loading, giving rise to a significant elongation of the specimen under test. The compression tests for the auxetic foam give results similar to other grey negative Poisson's ratio foams [9], with a Young's modulus of 105 kPa, lower than the corresponding one for conventional foams. It also showed that densification effects become important after engineering strains of 40 %.
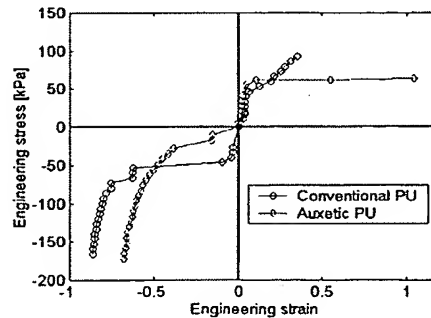
Fig. 2. Static tensile test results (tension and compression) of conventional and auxetic PU specimen

The remarkable difference in mechanical behaviour between conventional and auxetic foam was apparent for high constant strain loading. Figures 3 and 4 show the time histories of the auxetic and normal specimens, respectively. The auxetic specimens were loaded under a constant strain rate of $15s^{-1}$ [12]. It is evident that the auxetic samples clearly show a time-load history when subjected to dynamic crushing. In comparison, the normal open cell samples do not show any kind of noticeable resilience under high-strain rate loading. In Figure 4 one can notice that the load overshoot is due only to the load cell sensitivity when the upper plate of the cam plastometer approaches contact with the lower plate. Apart from this peak, only the sensor noise is recorded.
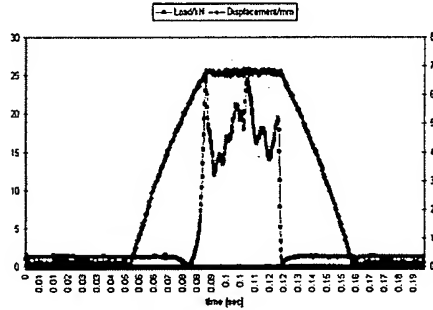
Fig. 3. Time history of displacement and reaction force recorded on the auxetic specimen
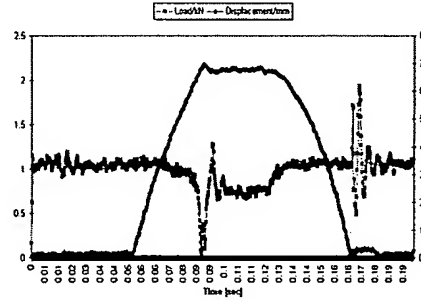
Fig. 4. Time history of displacement and reaction force recorded on the conventional rigid PU foam specimen

Figure 5 shows the experimental results of the auxetic foam samples under different constant strain rate values. The auxetic foam behaves in a similar manner to high-density foams under crush loading, with low sensitivity to different strain rate values [11]. This fact is explained by the manufacturing process used to convert conventional cellular solids into negative Poisson's ratio ones, involving multiple compressions to deform the unit cell and buckle its ribs [2, 4].

The data from the auxetic foams have been then processed to extract a stress-strain curve using the model suggested by Nagy *et al.* [14]. The experimental data were fitted with a polynomial of order 9, and then fitted to the following formula:

$$\sigma(\varepsilon) = \sigma_0(\varepsilon)\left(\frac{\dot{\varepsilon}}{\dot{\varepsilon}_0}\right)^{a+b\varepsilon} \tag{1}$$

Where $\sigma_0(\varepsilon)$ is a reference stress-strain curve and $\dot{\varepsilon}_0$ is the reference strain rate. The coefficients a and b were identified through a non-linear Least Square fitting technique. The reference strain rate $\dot{\varepsilon}_0$ was 1.43 s^{-1}. Figure 6 shows semi-empirical stress-strain relations found with Equation (1) for the different constant strain rates. One can notice the influence of the strain rate loading only during the densification phase in compression of the foam samples. At 38 s^{-1}, the stresses during the densification phase are higher compared to the ones at 15 s^{-1} but, for the case of 54 s^{-1}, the stress levels are comparable to the ones of the lower

constant strain rate value. The effect from the different strain rate loading is small and, at this stage, we are not able to give a full explanation of the phenomenon. We observe only that microinertia [13] and gas stiffening effects within the pores when considered as enclosed cavities [15] could contribute to the dynamic crushing loading behaviour of cellular solids.
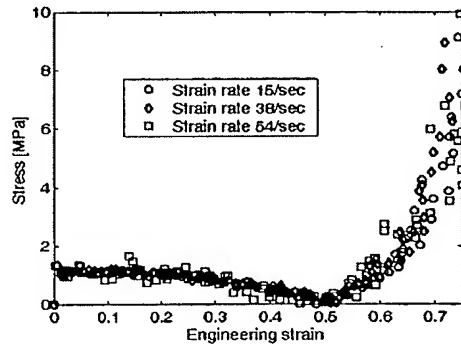

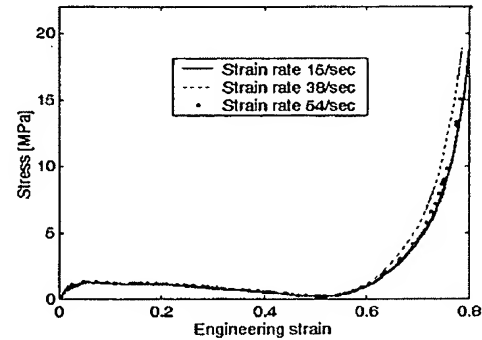Fig 5. Experimental stress-strain values for the auxetic foam specimen under different constant strain rate values.

Fig 6. Interpolated stress-strain curves Nagy's Law.

The MR seeded foam samplewas subjected to quasistatic pure tensile loading. Figure 6 shows the different behaviour of the foams under tensile loading, and their elastic recovery due to the particular manufacturing process. The MR fluid seeding gives rise to a slight scaling down of the tensile properties of the dry auxetic foam. In fact, the Young's modulus is decreased in this case to a value of 290 kPa, while the plateau stress is of 21 kPa. However, also in this case, the plateau region goes well beyond the rupture point of the conventional foam, and the MR seeded auxetic foam shows the same elastic force restoring characteristics of its dry version.
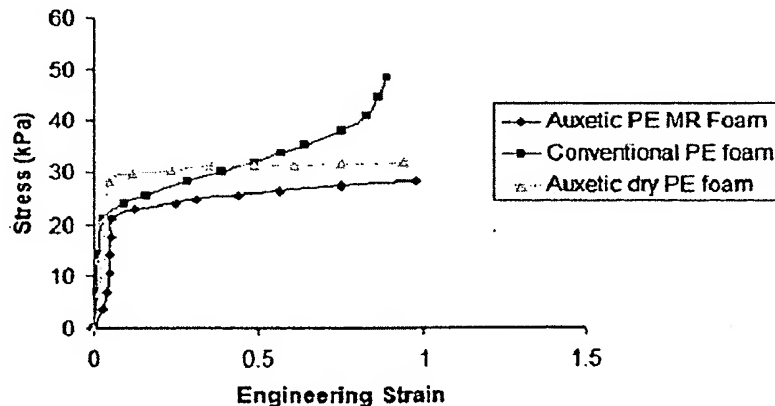
Figure 7. Comparison between the different foams subjected to pure tensile loading

3. ELECTROMAGNETIC PROPERTIES

The permittivity and permeability of four foam specimens has been measured at microwave frequencies. The foam specimens comprised a conventional rigid PU foam, two auxetic PU samples and one auxetic PU coated with the Lord MRF132 fluid. Measurements were taken over the band 12.4-18GHz, which encompasses the higher radar bands. Thus the foam measurements examine the suitability of the specimens as components in structural radar absorbers. Measurements were carried out using conventional S-parameter techniques, whereby the complex reflection and transmission coefficients relating to each specimen were measured and used to determine the permittivity and permeability of each specimen [16]. The measurements were carried out in rectangular waveguide having nominal transverse dimensions 23mm×11mm (these are also the sample dimensions). Measured permittivity and permeability data for the four specimens are shown in Figures 8-11.

The measured relative permittivity and permeability data for the PU foam specimens are similar to free space values (i.e. 1). These foams will therefore have little additional impact on an electromagnetic system and will not be used in applications that require simultaneously structural and electromagnetic performance. Data for the auxetic foam show an increased permittivity and permeability compared to the non-auxetic foams. Auxetic materials tend to have a higher relative density than non-auxetics [7-8, 12-13], a property that increases the relative permittivity of the material. The iron carbonyl in the MR fluid increases further the permittivity (and permeability) of the auxetic foam. Nonetheless, the relative values shown in Figures 8-11 for the MR specimen remain low compared to other dielectric and magnetic materials. The materials investigated in this study will have few applications; however, the sample properties were not optimized to achieve a desired electromagnetic effect and further developments in tailoring the foams' electromagnetic properties can be expected using alternative MR fluid mixtures.
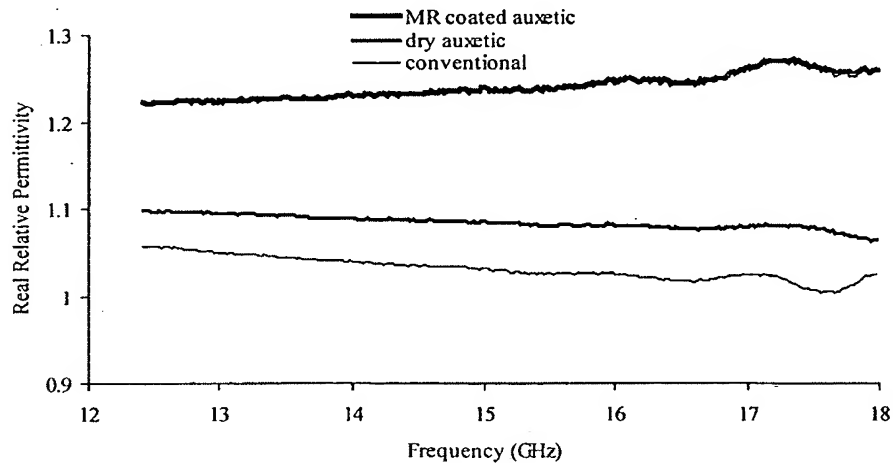

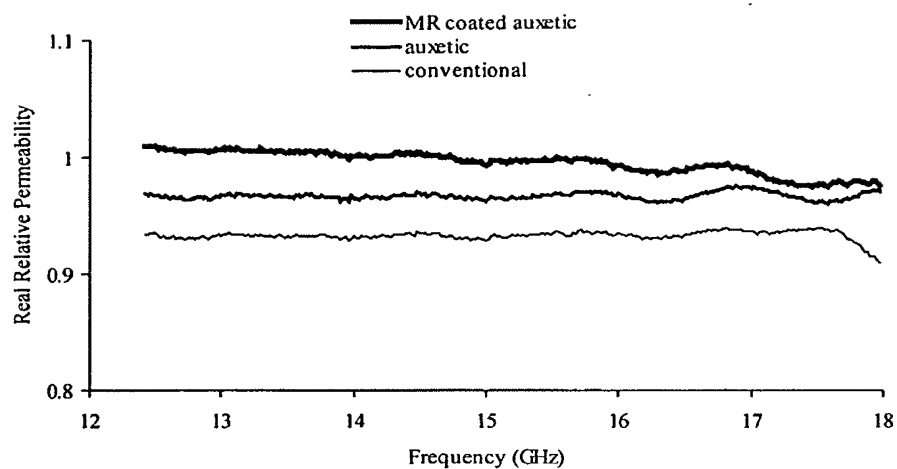Fig 8. Measured real part of permittivity of the four foam specimens

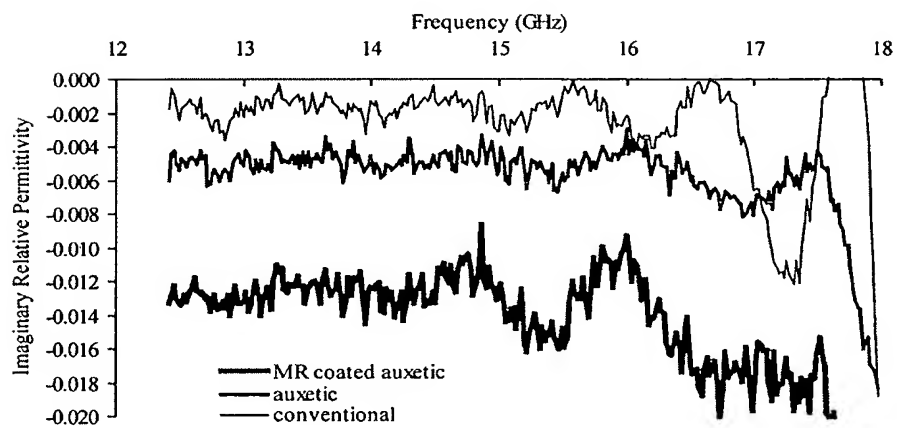Fig 9. Measured real part of permeability of the four foam specimens

Fig 10. Measured imaginary part of permittivity of the four foam specimens
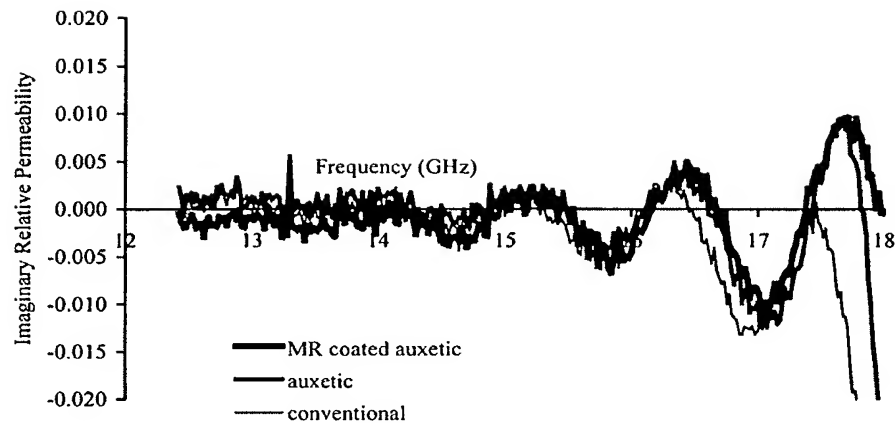
Fig 11. Measured imaginary part of permeability of the four foam specimens

4. CONCLUSIONS

In this paper a comparative experimental study on some mechanical and dielectric properties rigid polyurethane conventional and auxetic foams has been presented. A set of auxetic foams has also been seeded with magnetorheological fluid during the manufacturing process, in order to induce a coating on the external surface of the foam samples. The auxetic foams showed enhanced resilience under dynamic crushing loading and elongation capacity under pure tensile test up to 135 %, while the conventional foam had an ultimate load at 35 % of elongation. The presence of the MR fluid coating affected the tensile behavior with surface effects, with a slight decrease in terms of yield stress, but the long plateau area originated by the unfolding of the ribs was maintained. The auxetic foam samples showed an increase in terms of relative permittivity, also because of their increase in terms of relative density. The presence of the iron particulate of the MR coating helped to increase substantially the EM properties of the auxetic foam.

ACKNOWLEDGEMENTS

REFERENCES

[1]   R S. Lakes, "Foam Structures with a Negative Poisson's ratio", *Nature*, Vol 253, 1038, 1987

[2]   K. E. Evans, "Auxetic polymers: a new range of materials", *Endeavour, New Series*, Vol 15 (4), 170, 1991

[3]   R S Lakes and K Elm, "Indentability of conventional and negative Poisson's ratio foams". *Journal of Composite Materials*, Vol 27, 119, 1993

[4]   R S Lakes, "Design considerations for negative Poisson's ratio materials", *ASME Journal of Mechanical Design* Vol 115, 696, 1993

[5] F Scarpa and P J Tomlin, "On the transverse shear modulus of negative Poisson's ratio honeycomb structures", *Fatigue and Fracture in Engineering Materials and Structures*, **23**, 717 (2000)

[6] F Scarpa and G Tomlinson, "Theoretical characteristics of the vibration of sandwich plates with in-plane negative Poisson's ratio values", *Journal of Sound and Vibration* **230** (1) 45 (2000)

[7] F C Smith and F Scarpa, "The Electromagnetic Properties of Re-entrant Dielectric Honeycombs", *IEEE Microwave and Guided Wave Letters*, **10** (11) 451 (2000)

[8] F. Scarpa, G. Burriesci, F. C. Smith and B. Chambers. Mechanical and dielectric properties of auxetic honeycomb structures. *The Aeronautical Journal*, **107**(1069), 175 (2003)

[9] E A Friis, R S Lakes and J B Park, "Negative Poisson's ratio polymeric and metallic foams", *Journal of Materials Science* **23** 4406 (1988)

[10] W. R Powers. US Patent 3 025 200 (1962)

[11] H. Mahfuz, W. Al Mamun and S. Jeelani, "High Strain Rate Response of Sandwich Composite: Effect of Core Density and Core Skin Debond", *SAMPE Journal of Advanced Materials*, **33** (1) (2002)

[12] F Scarpa, J.R Yates, L.G Ciffo and S Patsias, "Dynamic crushing of auxetic open cell polyurethane foam". Journal of Mechanical Engineering Science, *Proceedings of the Institution of Mechanical Engineers*, **216** Part C, 1153 (2002)

[13] L J Gibson and M F Ashby, "Cellular Solids: Structure and Properties", 2nd Edition, Cambridge Press, Cambridge, UK (1997)

[14] A Nagy, W L Ko and U S Lindholm, "Mechanical behaviour of foamed materials under dynamic compression", *Journal of Cellular Plastics*, **10**, 127 (1964).

[15] F. Scarpa, "Parametric Sensitivity Analysis of Coupled Acoustic-Structural Systems", *Journal of Vibration and Acoustics, Transactions of the ASME*, **122**, 109 (2000)

[16] Hewlett-Packard Product Note 8510-3, 'Materials Measurement — Measuring the Dielectric Constant of Solids with the HP 8510 Network Analyzer', 1985

[17] M. R. Jolly, J. W. Bender and J D. Carlson, "Properties and applications of MR fluids", *SPIE 5th International Symposium on Smart Structures and Materials*, San Diego, CA, 15 March, 1998.

EXHIBIT D

Negative Poisson's Ratio Polymeric and Metallic Foams

adapted from

ABSTRACT

Foam materials based on metal and several polymers were transformed so that their cellular architectures became re-entrant, ie. with inwardly protruding cell ribs. Foams with re-entrant structures exhibited negative Poisson's ratios as well as greater resilience than conventional foams. Foams with negative Poisson's ratios were prepared using different techniques and materials and their mechanical behavior and structure evaluated.

1. INTRODUCTION

1.1 Conventional Foams

Cellular solids, or structural foams, constitute a class of composite materials in which one phase is gaseous. Such foams are manufactured for a wide variety of applications; moreover, cellular solids occur in nature, eg. wood and bone. Foam materials may be classified as open cell, in which the interior of each cell communicates with the outside atmosphere; closed cell, in which each cell is sealed by cell walls; and mixed, in which both open and closed cells are present. The mechanical properties of foams are determined by the properties of the parent solid material; the volume fraction of solid material, equivalent to the relative density ρ_{foam}/ρ_{solid}; and the cell structure. As for the cell structure, the cells of most man-made polymer foams have a shape which can be modelled by the Kelvin minimum area tetrakaidecahedron [1]. This polyhedron, depicted in Fig. 1, is convex and has eight curved hexagonal faces and six curved square faces. The mechanical properties of foams can, however, be modelled using simple structural arguments in which the dominant deformation mode is assumed to be the bending of the cell ribs, combined with empirical determination of scaling constants [2,3]. Many mechanical properties can be successfully predicted by such an approach. In this article we are concerned principally with Young's modulus and Poisson's ratio. The modulus of elasticity E of open cell foams is given in terms of the density of the solid phase ρ_{solid} and the density of the foam ρ_{foam}, by

$$E_{foam}/E_{solid} = [\rho_{foam}/\rho_{solid}]^2 . \tag{1}$$

Many closed cell foams have very thin cell walls and most of the material is in the ribs. Such foams also follow Eq. 1. Poisson's ratio based on this foam theory is given, for all densities, by

$$\nu = 0.33. \tag{2}$$

The plastic collapse stress σ_{pl} for a foam in which the cell ribs yield (at a stress β_y), is given, for relative density less than 0.3, by

$$\sigma_{pl}/\sigma_y = 0.3 \, [\rho_{foam}/\rho_{solid}]^{3/2}. \tag{3}$$

This article deals with foam materials with cell structure which differs considerably from that of the conventional foams considered in [2,3].

1.2 Re-entrant Foams

Nearly all ordinary materials, including foams, exhibit a positive Poisson's ratio, that is, they become smaller in cross section when stretched and larger when compressed.

Theoretically, however, negative Poisson's ratios are permissible. In particular, the allowable range of Poisson's ratio for an isotropic material is -1.0 to +0.5 [4]. Recently, one of the authors reported a new class of foam materials which exhibits a negative Poisson's ratio as well as other characteristics such as enhanced resilience [5,6]. These materials were produced by transformation of a conventional foam so that the cell ribs protrude inward rather than outward: a 're-entrant' structure. Fig. 2 displays an idealized re-entrant unit cell. To visualize the relationship between structure and Poisson's ratio, imagine tension to be applied to the vertically protruding ribs. The ribs in the lateral directions will tend to move out, causing lateral expansion. When compression is applied, the ribs, which are already curved inward, will bend inward further, thus resulting in lateral contraction in response to axial compression.

The technique for creating the re-entrant structure is to apply, by some method, permanent compression in three orthogonal directions. A foam with relatively low volume fraction of material must be used such that buckling of ribs may occur. Two methods were found suitable for creating re-entrant cell structures [5,6]. For thermoplastic polymer foams, the procedure entails triaxial compression by a factor of 1.4 to 4 in volume, followed by heating to a temperature above the softening point, followed by cooling under the volumetric constraint. For metallic foams made of ductile metal, the procedure consists of applying uniaxial compression at room temperature until the foam yields. Additional compressions are applied sequentially in each of three orthogonal directions until the desired volume change is achieved. The thermal transformation technique used on thermoplastic foams would, in principle, be applicable for metal foams. However, difficulty may be experienced due to the high, sharp melting point of such materials.

Re-entrant foams were found to be more resilient than conventional foams. Conventional foams typically exhibit an approximately linear compressive stress-strain curve up to about 5% strain [2,3]. Re-entrant foams exhibit a nearly linear relationship between stress and strain up to about 40% strain, depending on the amount of permanent compression applied in transformation [5,6]. A similar improvement in resiliency has been reported in foams with permanent uniaxial compression [7], but these foams do not exhibit a negative Poisson's ratio [5,6].

No restriction is imposed on the size of the cell structure since the theory of elasticity has no length scale. In principle, low density foams with microstructure on a scale smaller than one micron [1 μm] could be transformed to re-entrant structures with a negative Poisson's ratio [5].

Several other examples of materials exhibiting a negative Poisson's ratio are known. A "single crystal", possibly a twinned crystal, of pyrite with a Poisson's ratio of -0.14 was recognized by Love [8]. Other examples of a negative Poisson's ratio are in anisotropic single crystal cadmium in some directions [9] and in anisotropic, macroscopic two-dimensional flexible models of certain honeycomb structures (not materials) in some directions [3]. These examples, however, all exhibit a high degree of anisotropy; the negative Poisson effect only occurs in certain directions and then may be dominated by coupling between stretching force and shear deformation. An additional example of a structure with a negative Poisson's ratio is a framework of rods, hinges, and springs [10].

The objectives of this study were to develop and evaluate techniques transforming polymer and metal foams into materials with re-entrant microstructures.

2. MATERIALS AND METHODS
2.1. Sample Preparation
2.1.1 Thermoplastic Foam Transformation

Polyester urethane foam of solid volume fraction 0.043 was used for this segment. The method used was to pack the foam into a square cross section aluminum tube 22 mm by 22 mm in interior dimensions, such that an approximately equal compression in each of three orthogonal directions was applied to the sample. This tube was heated at 200°C in a

tubular furnace for approximately seven minutes and cooled to ambient temperature. Several such specimens were prepared. The permanent volumetric compression ratio in the material reported here was 3.4.

2.1.2 Thermosetting Foam Formation and Transformation

In this study, a RTV (room temperature vulcanizing) elastomeric silicone foam was chosen as a representative sample of a thermosetting polymeric foam. It was obtained from the manufacturer [11] as a two part mixture. Specific mixing instructions of the ingredients (silanol-terminated polymers, a cross-linking agent, a catalyst, and a foaming agent) were followed as recommended by the manufacturer. A 10:1 ratio of elastomer base to catalyst and a mixing time of 30 seconds were used. According to the manufacturer, foaming is completed in about 3 minutes and the material is fully cured in about 24 hours. In order to provide adequate mixing, a common paint stirrer inserted in a 3/8 inch hand held electric drill was used to stir the preparation during the initial foaming process. Following the initial 30 seconds of mixing, the foaming mixture was poured into a container and allowed to continue to foam and expand freely. Foaming continued for approximately 2 minutes. This conventional foam had a solid volume fraction of 0.14.

A method was developed in which the foam was mixed as usual and allowed to completely foam and set for anywhere from 15 to 30 minutes before triaxial compression was applied. Triaxial compression was accomplished using a custom made device. Plexiglas® plates coated with petroleum jelly were used to reduce the constraining force along the plates parallel to the direction of the applied compression. Compressions ranging from 10% to 40% strain in each direction were applied to various samples. The re-entrant foam reported here had a permanent volumetric compression ratio of 2.0.

2.1.3 Metal Foam Preparation

A 4x4x2 inch block of copper foam with a pore size of about 1 mm and solid volume fraction 0.053 was obtained from a manufacturer [12]. The copper foam was transformed into re-entrant foam by successive applications of small increments of plastic deformation in three orthogonal directions. A vise was used to apply the deformation. Plexiglas® sheets with coarse sandpaper covers were used to make an even surface on the faces of the vise. Several samples of compressed foam were prepared with strains of 20-35% in each of three orthogonal directions. The material reported here had a permanent volumetric compression ratio of 1.73.

2.2 Testing Methods
2.2.1 Mechanical Tests

Tensile tests were performed on polymeric foam samples on a servo-hydraulic materials testing machine (MTS Model 812, MTS Systems Corp.; Minneapolis, MN). Special end attachments were devised in accordance with ASTM Standards [13]. These attachments allowed for elimination of bending moment through the universal joint such that pure tension was applied. Specimens were cemented onto the surfaces of the testing devices. A cyanoacrylate adhesive was used for the polyester foams and Duco® cement was used for the silicone foams. Special care was taken to ensure that the specimens were centered directly with the line of action of the ram of the machine. A strain rate of 0.008 /second was used. The specimens were made geometrically similar so that changes in strain with time would be similar for all samples. Load versus displacement curves, as plotted by the MTS x-y recorder, were obtained for all samples. Engineering stress strain curves were derived from these data.

Uniaxial compression tests were performed using the MTS materials testing machine on various samples of re-entrant and conventional copper foam. Specimens were cut into geometrically similar pieces using a diamond saw (Low Speed Isomet, Model 11-1180, Buehler LTD, Lake Bluff, IL) under water irrigation. Short, stubby samples were cut for compression tests. In compression testing, a special tilting compensation plate and end

lubrication were used in accordance with ASTM Standards [14]. An initial strain rate of .010/min was utilized for both compression tests.

Load-displacement curves for were recorded for all mechanical tests and high magnification video tapings of the tests were taken for future use in measuring Poisson's ratios.

2.2.2 Data Reduction and Measuring Poisson's Ratio

For all samples tested, engineering stress-strain graphs were made from load displacement data. The graphs generally exhibited a bilinear form, therefore, elastic moduli for the Silastic® foam samples were measured for different regions of strain. E_1, which corresponds to a Young's modulus, was measured as the slope of the stress-strain curve in the region of just above zero to 1.5% strain and E_2, corresponding to a tangent modulus, was measured as the slope in the region of 3.5% to the final strain.

The Poisson's ratios of all samples tested was determined by viewing the high magnification video tapes of the tensile tests and measuring the displacements in both axial and transverse directions simultaneously. Other methods of measuring Poisson's ratio which comply with ASTM Standards [15] were tried and found unsuitable due to the inherently rough, porous surface of the foams.

2.3 SEM Evaluation of Foams

Scanning electron micrographs of re-entrant and conventional foams were taken at low magnifications to display the coarse cell structure. Accelerating beam voltages were 15 kV for the polyester and copper foams and 8 kV for the silicone rubber foams. The polyester and silicone rubber foams were sputter- coated with AuPd; the copper foams, being electrically conductive, did not require coating. Micrographs of polyester foam were taken of a re-entrant sample, a re-entrant sample in a state of tensile strain of approximately 40%, and the conventional foam. Micrographs of re-entrant and conventional copper and silicone rubber foams were also taken.

3. RESULTS AND DISCUSSION

3.1 Mechanical Tests

Figures 3-6 show that typical stress-strain curves for the thermosetting, thermoplastic, and copper foams. Table 1 contains a summary of the tensile tests of the Silastic® foam shown in Figure 3, as well as results dealing with the anisotropy of Poisson's ratio measured in different directions. Observe that the elastic moduli (E_1 and E_2) for the re-entrant foams are much lower than for the conventional foam control. It was found that 25% permanent axial strain (which corresponds to about a factor of 2 permanent volumetric compression ratio) yielded the best results for silicone rubber foams. Both re-entrant samples had a substantial negative Poisson's ratio and the difference between the values can be accounted for by the nonuniformity of the original foam structure. The conventional control sample had a Poisson's ratio of around +0.5. Typical foams have a Poisson's ratio of +0.3 ± 0.1. The anisotropy of the foam would account for the abnormally high Poisson's ratio.

Figure 4 is a tensile stress-strain graph of conventional and re-entrant polyester polyurethane (thermoplastic) foams. The conventional foam had a solid volume fraction of 0.043 and exhibited a Poisson's ratio of about +0.4. The re-entrant foam had a permanent volumetric compression ratio of 3.4 and a Poisson's ratio of -0.4. The increased resilience of the re-entrant foam is evident from the curves shown in Fig. 4.

Analysis of compressive tests on re-entrant and conventional copper foams yielded the stress-strain curves given in Figure 5. The conventional foam had a solid volume fraction of 0.053. The re-entrant sample had a permanent volumetric compression ratio of 1.7. As can be seen from Figure 6, a graph of the small strain region of the stress-strain curve, the re-entrant foam was less stiff than the conventional foam. The conventional copper foam

exhibited a Poisson's ratio of about +0.42, typical for a foam material. In contrast, the re-entrant copper foam exhibited a Poisson's ratio of -0.39 in the initial stages of compression with progressively increasing values as the magnitude of axial strain increased.

The mode of deformation in the copper foam may be elucidated by evaluation of the plastic collapse stress of the conventional foam and comparison of this value with values predicted from the theory of cellular solids for different deformation modes. By use of Equation 3, which predicts the plastic collapse stress of foams which yield, it was found that the predicted plastic collapse stress differed from the observed plastic collapse stress of copper foam by only a factor of 1.2. The ideal foam theory predicts the major mode of deformation in the copper foams to be by plastic hinge formation. Microscopic examination of re-entrant foam structures, however, suggests that plastic buckling of the ribs also occurs.

3.2 SEM Results

Figure 7 shows the micrograph of the conventional polyester foam sample. The cells in this foam are rather round and symmetrical, similar to the ideal cell structure shown previously in Figure 1. In contrast, the cells of the re-entrant foam, shown in Figure 8, are convoluted and buckled, depicting the typical re-entrant structure. Figure 9 displays re-entrant foam under tension. The underlying kinematics responsible for the negative Poisson's ratio may be visualized from this micrograph. In comparison to the ribs of the cells in the unstrained re-entrant foam of Figure 8, the cell ribs of the strained re-entrant foam are straightened outward and the resulting cell structure is more similar to that of the conventional foam.

It can also be seen from Figures 7-9 that the polyester foam is actually a part closed, part open cell structure. The cell walls, however, appeared to be nearly translucent under optical microscopic examination and were very thin. This finding confirms the supposition [2,3] that man-made foams, even if closed cell in nature, often behave as an open-cell foam. Figure 9 shows a sample in a strained state: many of the cell walls have been torn or ruptured yet the ribs were intact. This observation supports the idea that the ribs are of greater mechanical importance than the walls in such foams.

SEM micrographs of a typical conventional and re-entrant Silastic® foam are shown in Figures 10 and 11, respectively. In the micrograph of the conventional foam in Figure 10, one can see from the relative thickness of the ribs that the Silastic® foam has a much higher solid volume fraction in comparison with the polyester foam shown in Figure 9, in agreement with the quantitative measurements of density described above. Also illustrated in Figure 10 is the nonuniformity in pore size. These two observations would indicate that this Silastic® foam might not respond to the transformation technique as well as some other lower density, more uniform foams such as the polyester foam. Figure 11 shows the re-entrant Silastic® foam after a permanent triaxial compression of approximately 25%. As one can see from Figure 11, the Silastic® re-entrant foam does exhibit a re-entrant type structure, however, this structure is not as clear and defined as with the lower density polyester re-entrant foams. This finding corresponds to the previous observation that the higher relative density Silastic® re-entrant foams do not exhibit as negative a Poisson's ratio as the lower density polyester re-entrant foams.

Figures 12 and 13 show micrographs of the conventional and re-entrant copper foam, respectively. From these pictures, one can see the typical strut-buckled re-entrant structure illustrated in the re-entrant copper foam. Also seen in this foam, however, are the deformations of the 'hinges' between the ribs. The SEM photographs thus provide verification of the predictions of foam theory.

## 4. CONCLUSIONS

We draw the following conclusions.

1. Three methods are successful in transforming conventional foams to re-entrant foams. These methods are: triaxial compression followed by heat treatment for thermoplastic polymer foams; triaxial compression during the foaming process for thermosetting polymer foams; and sequential plastic compression in three directions for metal foams.

2. Re-entrant foams exhibited negative Poisson's ratios and had Young's moduli which were smaller than those of conventional foams.

3. Re-entrant polymer foams were more resilient than the corresponding conventional foams.

4. Re-entrant transformation of metal foam involves both plastic hinge formation and plastic buckling of the cell ribs.

REFERENCES

1. H. A. Lanceley, J. Mann, G. Pogany, "Thermoplastic systems", pp. 221-289 in "Composite Materials", ed, L. Holliday, Elsevier, Amsterdam, (1966).
2. M.F. Ashby, *Metallurgical Transactions,* 14A (1983) 1755.
3. L.J. Gibson, M.F. Ashby, G.S. Schajer, and C.I. Robertson. *Proc. R. Soc. Lond.* A382 (1982) 25.
4. Y.C. Fung, "Foundations of Solid Mechanics" p. 353, Prentice-Hall, Englewood Cliffs, NJ, (1968).
5. R.S. Lakes; *Science* 235 (1987) 1038.
6. R.S. Lakes, U. S. Patent # 4,668,557, (1987).
7. W.R. Powers, U.S. Patent 3,025,200 (1962).
8. A.E.H. Love, "A Treatise on the Mathematical Theory of Elasticity" p. 163, 4th Ed.(Dover, New York, 1944).
9. Y. Li, *Phys. Status Solidi.* 38 (1976) 171.
10. R. F. Almgren, *J. Elasticity* 15 (1985) 427.
11. Dow Corning Corp. Midland, MI.
12. Astro Met Associates, Inc. Cincinnati, OH.
13. Annual Book of ASTM Standards."Standard Test Method for Rubber Properties in Tension" (1984) Designation: D412-83.
14. Annual Book of ASTM Standards."Standard Methods of Compression Testing of Metallic Materials at Room Temperature" (1984) Designation: E9-81.
15. Annual Book of ASTM Standards."Standard Test Method for Poisson's Ratio at Room Temperature", (1984) Designation: E132-61.
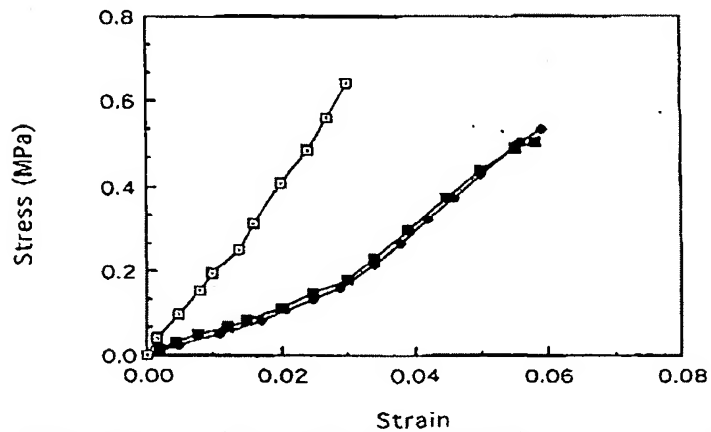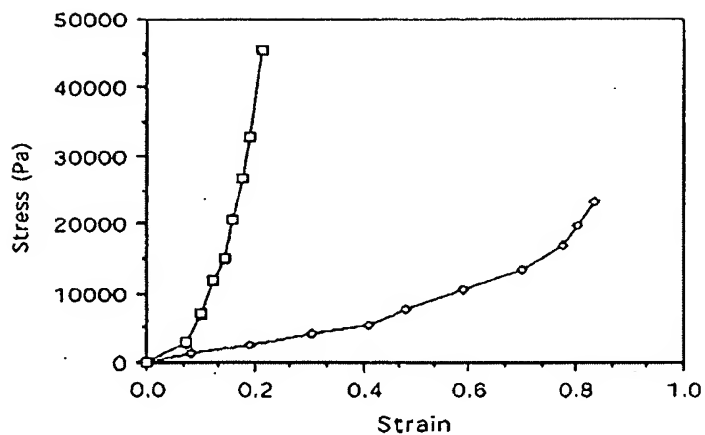
FIGURES
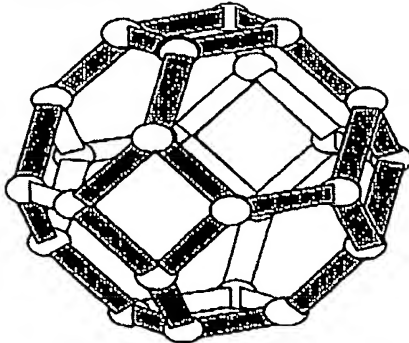
1.   Idealized unit cell of conventional foam.
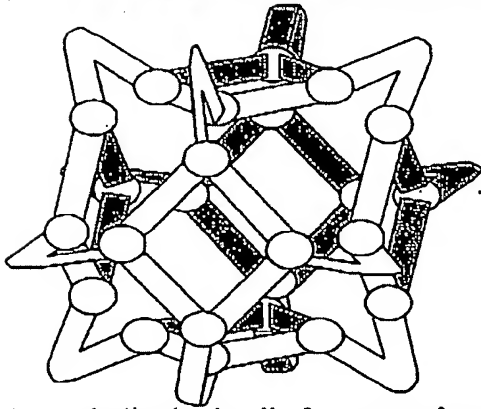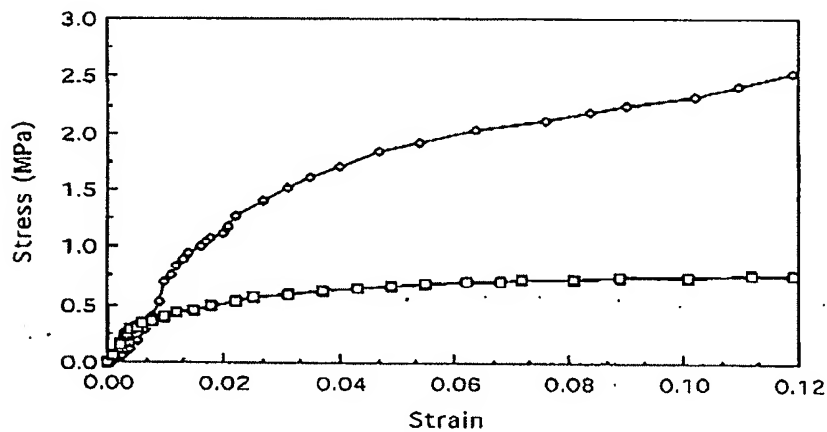

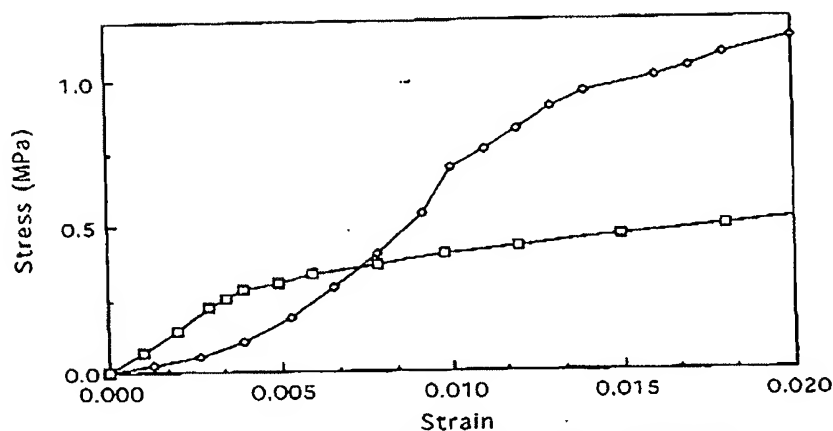2.   Idealized unit cell of re-entrant foam.

3.   Tensile stress-strain curves for conventional and re-entrant silicone rubber foams.
      Squares: conventional foam. Solid volume fraction: 0.14.
      Solid symbols: two specimens of re-entrant foam.
      Permanent volumetric compression ratio: 2.0

4. Tensile stress-strain curves for conventional and re-entrant polyurethane foams.
Squares : conventional foam. Solid volume fraction: 0.043.
0: re-entrant foam. Permanent volumetric compression ratio: 3.4.

5. Compressive stress-strain curves for copper foams.
squares: conventional foam. Solid volume fraction: 0.053.
0: re-entrant foam. Permanent volumetric compression ratio: 1.7.

6.   Initial region of compressive stress-strain curves for copper foams.
squares: conventional foam. Solid volume fraction: 0.053.
◊: re-entrant foam. Permanent volumetric compression ratio: 1.7.

7.   Scanning electron micrograph of conventional polyester foam.
Solid volume fraction: 0.043.   For these see the original article.
8.   Scanning electron micrograph of re-entrant polyester foam.
9.   Scanning electron micrograph of re-entrant polyester foam stretched vertically.
10.   Scanning electron micrograph of conventional silicone rubber foam. Solid volume
fraction: 0.14.
11.   Scanning electron micrograph of re-entrant silicone rubber foam.
12.   Scanning electron micrograph of conventional copper foam.
           Solid volume fraction: 0.053.
13.   Scanning electron micrograph of re-entrant copper foam.

ACKNOWLEDGMENT

Table 1. Tensile test results for re-entrant and control Silastic® foams.

Specimen	Permanent Strain(%)			Modulus of Elasticity (MPa)		Poisson's Ratio			Density (g/cm³)
	ε_x	ε_y	ε_z	E_1	E_2	ν_1	ν_2	ν_3	ρ
Control	0	0	0	17.38	26.00	0.58	0.43	0.47	0.15
Re-entrant	28.6	24.4	25.6	4.78	11.83	-0.19	-0.25	-0.15	0.30
Re-entrant	28.6	24.4	25.6	4.33	13.30	-0.09	-0.05	-0.03	0.25